Poly-L-Lysine modified Iron oxide nanoparticles: Synthesis, characterization and antimicrobial properties

A THESIS SUBMITTED BY

Athira Devi J S

To

SREE CHITRA TIRUNAL INSTITUTE FOR MEDICAL SCIENCES AND TECHNOLOGY

THIRUVANANTHAPURAM

INDIA

IN PARTIAL FULFILMENT OF THE REQUIREMENTS

FOR THE AWARD OF

MASTER OF PHILOSOPHY

IN

BIOMEDICAL TECHNOLOGY

2021

DECLARATION

I, AthiraDevi J S, hereby certify that I had personally carried out the work depicted in the thesis entitled,**"Poly-L-lysine modified Iron oxide nanoparticles: Synthesis, characterization and antimicrobial properties"**except where due acknowledgment has been made in the text. No part of the thesis has been submitted for the award of any other degree or diploma prior to this date.

Thiruvananthapuram
19-07-2021

Athira Devi J S
Reg. No: 2020/MPHIL/05
Roll No: 7781

SREE CHITRA TIRUNAL INSTITUTE FOR MEDICAL SCIENCES & TECHNOLOGY

Thiruvananthapuram – 695011, INDIA

(An Institute of National Importance under Govt. of India)

Phone-(91)0471-2520273 Fax-(91)0471-2341814

Email: jayasree@sctimst.ac.in

Web site :www.sctimst.ac.in

CERTIFICATE

This is to certify that **Ms. Athira Devi J S**, in the Division of Biophotonics and Imaging of this institute has fulfilled the requirements prescribed for the MPhil degree of the Sree Chitra Tirunal Institute for Medical Sciences and Technology, Thiruvananthapuram. The thesis entitled, ***"Poly-L-lysine modified Iron oxide nanoparticles: Synthesis, characterization and antimicrobial properties"*** was carried out under my direct supervision. No part of the thesis was submitted for the award of any degree or diploma prior to this date.

Thiruvananthapuram

19-07-2021

Dr. R. S. Jayasree

(Research Supervisor)

Scientist 'F'

Division of Biophotonics & Imaging

BMT Wing, SCTIMST

Thiruvananthapuram

The thesis entitled

"Poly-L-lysine modified Iron oxide nanoparticles: Synthesis, characterization and antimicrobial properties"

Submitted by
Athira Devi J S

For the degree of
Master of Philosophy
of

SREE CHITRA TIRUNAL INSTITUTE FOR

MEDICAL SCIENCES & TECHNOLOGY

Thiruvananthapuram – 695011

is evaluated and approved by

.....	.....
Dr. R S Jayasree Scientist 'F' Division of Biophotonics & Imaging SCTIMST	Examiner

ACKNOWLEDGEMENTS

In the preparation of this project work, I have been received guidance, assistance, open handed help, and benevolent support from a magnitude of people. Without their assistance and well wishes, this work could not have materialized. Hence, let me take this opportunity to extend my wholehearted gratitude to all of them.

At first, I feel immensely fortunate to express my massive indebtedness and profound gratitude to my guide and supervisor Dr. R S Jayasree, who offered continuous advice, constant encouragement, inspiring discussions, and valuable suggestions to do this work with confidence. I am thankful for all the moral support and help she has given me during the entire course of my M Phil work. I owe my sincere gratitude to The Director, SCTIMST and Head BMT Wing for providing the infrastructural facilities. I extend my thanks to Dean, Registrar, Deputy Registrar and everyone in the academic division for their kind support and help.

I am indebted to Dr. Anoop Kumar T, Dr R S Jayasree and Dr. Francis Fernandez, our course coordinators, for providing me this opportunity to be a part of the MPhil group. I am also thankful to all faculty members who have painstakingly delivered excellent classes for our M.Phil course work.

I am thankful to Dr. Maya Nandkumar A, Division of Microbial Technology for helping me to complete the crucial antimicrobial studies for this work. I am also grateful to Dr. Anilkumar P R, Division of Tissue Culture for his help and support in providing cell culture facilities and allied studies.

I am grateful to Dr. Rekha M R, Division of Biosurface Technology, Dr. Manoj Komath, Division of Bioceramics and Dr. Lynda V Thomas, Division of Tissue Engineering and Regeneration Technologies for providing the DLS, TEM and FTIR facilities respectively.

I thank all the staffs in Central Laboratory for Instrumentation and Facilitation (CLIF), Karyavattom, Thiruvananthapuram, for providing XRD facility.

I am immensely thankful to the Ph.D scholars and technical staffs especially, Mrs. Linju M C, Miss. Evelyn and Miss. Susan Mani for their open-handed help.

On personal note, I would like to thank to Dr. Rekha C R (Research Associate), without her timely assistance and encouragement, this work would not have been a success. I extend my sincere gratitude to each and every member of Division of Biophotonics and Imaging, especially Mr. Dushyandhun, Mrs. Reshmi A N, Mr. Jijo PT, Miss. Anjana R S, Dr. Jibin K, and Mr. Sarathkumar E, for their friendly support and helping hands throughout my project.

Thanks to the staff of various administrative departments and library of the institute, security staff and cleaning staff for their kind support.

I would also like to thank all my MPhil mates and all other friends for their encouragement.

Above all, I owe a deep sense of gratitude to my parents, my brother and my dear and near one, for their everlasting encouragement and support to pursue and complete this work in an eminent way.

Last, but not at least, I express my sincere gratitude to the force of nature which guided me all this way.

Athira Devi J S

TABLE OF CONTENTS

LIST OF FIGURES

LIST OF TABLES

LIST OF ABBREVIATIONS

^{o}C	Celsius
AB	Antibiotic
AMP	Antimicrobial peptide
ATP	Adhenosine Triphosphate
CV	Crystal Violet
DLS	Dynamic Light Scattering
DNA	Deoxyribo Nucleic Acid
EPS	Extracellular Polymeric Substance
FTIR	Fourier Transform Infrared Spectroscopy
GoF	Goodness of fitting
H_2O_2	Hydrogen peroxide
IC50	Half-maximal Inhibitory Concentration
IONPs	Iron oxide nanoparticles
IONzyme	Iron oxide nanozyme
JCPDS	Joint Committee on Powder Diffraction Standards
mg	Milligram
MRI	Magnetic Resonance Imaging
MTT	3-(4, 5-Dimethylthiazol-2-yl)-2,5-diphenyltetrazolium bromide
mV	Milli Volt
nm	Nanometre

PLL	Poly-L-lysine
ROS	Reactive Oxygen Species
SPIONs	Super paramagnetic iron oxide nanoparticles
TEM	Transmission Electron Microscopy
TSB	Tryptone Soya Broth
XRD	X-Ray Diffraction
µg/ml	Microgram/Millilitre

SYNOPSIS

In the healthcare sector, bacterial colonization and biofilm formation is a considerable concern. It is well known that the primary cause of more than 70% of the hospital related complications and 80% of the infection associated deaths are due to the formation of biofilms. Majority of biofilm infections are found in teeth, lungs, skin, heart and the urinary tract. Medical implants and wounds are very susceptible to infections by *Staphylococcus aureus* and *Staphylococcus epidermidis*.*Staphylococcus* is responsible for most of the hospital acquired pneumonia cases. The gram-negative bacterial species such as *Escherichia coli, Klebsiella pneumoniae, and P. aeruginosa* are multidrug resistant strains which cause most of the infections in acute care facilities. Some of the device-related biofilm infections are mainly occurred in catheters, prosthetic joints, pacemakers and heart valves, contact lenses, orthopedic implants and so on. The bacteria in the biofilm act as a source for a wide range of infections. Once infected by any of these pathogens, the only solution is to permanently remove or replace the implant.

Development of novel antimicrobials and antibiofilm surfaces to protect the medical devices from the attack of antibiotic resistant strains is one of the very urgent needs. Recent developments in nanotechnology offers so much opportunities in synthesizing new biomaterials and surfaces with antimicrobial action. For most of the applications associated with antimicrobial mechanism, metal-based nanoparticles are of primary interest because of their intrinsic characteristics such as structural and electrochemical properties due to quantum confinement. Among these, magnetic nanoparticles are the most explored metallic nanoparticles. Magnetic nanoparticles exhibit different properties from bulk materials. In bulk materials, there are regions called magnetic domains. Within these domains magnetic moments are arranged. When the size is

reduced significantly, to nanolevel, the materials reach a condition in which only one domain exist and the magnetic and other surface properties changes drastically. These changes occurring in nanolevel is utilized for the various medical applications.

With these backgrounds, the objective of this thesis is to synthesize a polymer coated nanomaterial which offers antibacterial and antibiofilm properties. The work summarizes the synthesis, characterization and study of antibacterial properties of super paramagnetic iron oxide nanoparticles (SPIONs) modified by Poly-L-lysine (PLL). The thesis has been organized into five chapters. Chapter 1 provides a general introduction about the significance of nanotechnology in biomedical field, current problems related to bacterial-associated infections and biofilm formation, approaches to biofilm control, advantage of using iron oxide nanoparticles and influence of biopolymer coating on iron oxide nanoparticles. An overview on using iron oxide nanoparticles rather than other metal oxide nanoparticles is also provided.

Chapter 2 outlines the review of available literature on recent developments in nanotechnology for antibacterial treatments and the various applications of PLL and other biocompatible polymer coated iron oxide nanoparticles. This chapter also summarizes the need for developing antibacterial and antibiofilm surfaces to prevent the wide range of infections.

Chapter 3 elaborates the materials and methods employed for the synthesis of PLL modified SPIONs. In the first section, materials used for the synthesis are listed. The methods are briefly explained in the second part. The characterization techniques used are explained in this section. Various techniques adopted for material characterization are x-ray diffraction (XRD), Fourier transform infrared spectroscopy (FT-IR), transmission electron microscopy (TEM), dynamic light scattering technique (DLS) and zeta potential analysis. The SPIONs are prepared

via chemical co-precipitation method. The SPIONs obtained were modified with PLL. The nanoparticle synthesis was done as per existing protocols. In the next sub-section, cellular interaction studies, including cell viability and cytotoxicity evaluation were carried out using MTT assay. Oxidative damage upon exposure to the synthesized nanoparticles was determined spectrophotometrically using DCFH-DA assay.

Chapter 4 deals with the results and discussion of all the experiments done in the thesis. The first section covers the results obtained from nanoparticle synthesis followed by the detailed results obtained from various characterization techniques. The nanoparticles with spherical morphology showed an average size of about 15nm. The particle size was confirmed from XRD and TEM data. The synthesized nanoparticles are found to have excellent magnetic properties. In the next section, initial cytotoxicity studies for the optimization of concentration of synthesized nanomaterials were evaluated using MTT assay with L929 cell line. The inferences from all the experiments along with all possible theoretical interpretations are also done in this chapter.

In the sixth chapter, summary and conclusion of the work are discussed. The PLL modified SPIONs have successfully synthesized and characterized. The study mainly focused on understanding the efficiency of material to utilize it as an antimicrobial agent. The synthesized nanoparticles showed a dose-dependent cytotoxicity on incubation with L929 cells. Half maximal inhibitory concentration value of the nanoparticles is evaluated and the concentration is optimized. As a preliminary attempt, the effect of synthesized nanoparticles on biofilm formation was evaluated using a concentration of 25µl. Low level concentration did not show antibiofilm formation property for both gram-positive and gram-negative bacteria. However, the nanomaterials showed encouraging results on the biofilm disruptive property on biofilm formed after 48 hrs. The future prospects of the present work is also discussed in this section.

CHAPTER 1

INTRODUCTION

1.1 Nanotechnology in medicine

Nanotechnology is the study and application of materials at nanolevel which encompasses the fundamental research areas in physics, chemistry and biology. It has revolutionized many sectors such as medicine, information technology, biomedical industries etc. Materials whose size ranges from 1-100 nm which are either in aggregate form or in unbounded form are termed as nanomaterials. The particle size distribution and surface properties of nanomaterials greatly impact their properties and the applications. Reduction in particle size leads to high surface area to volume ratio. This makes nanomaterials much more reactive than their bulk counterparts. Nanotechnology applied for medicinal purposes is termed as 'nanomedicine', which is defined as the use of nanomaterials in monitoring, diagnosis, prevention and treatment of diseases (Tinkle *et al*., 2014). Nanomaterials applied in medical purposes are in three areas: nanotherapy, nanodiagnosis and regenerative medicine. Nanoparticles have been recognized as efficient diagnostic imaging materials such as fluorescent-labelled particles, magnetic resonance imaging and so on. Thus the development in nanotechnology has enabled to address several unmet medical needs.

For medicinal purposes, it is important to know how nanomaterials interact with biological fluids. A correct knowledge of the molecular processes will provide an understanding of designing the nanoparticles to target a specific location in the body (Louro *et al.,* 2018). The interaction between the surroundings of biological fluids and nanomaterials is also a concern. Most

commonly used nanomaterials for medicinal purposes belong to metals, metal oxides, polymeric composites or responsive smart nanomaterials. One of the most desirable properties of such nanomaterials is antibacterial property along with least toxicity. This property not only can accomplish its function inside the human body with no harm to system itself but also could be used as a preventive or therapeutic agents against microbial challenges like biofilms. Though nanomaterials offer a wide range of biomedical applications, researchers are so keen in improving the antimicrobial properties of nanomaterials and developing novel biomaterials.

1.2 Biofilm

A biofilm is an assembly of microbial cells that is irreversibly associated to a surface. Biofilm may form on living tissues, indwelling medical devices, water system piping and aquatic environments. A bacteria can exist in two different forms: planktonic state and sessile state. Planktonic state is the free-floating state and in the sessile state bacteria adhere to surface. The free-floating bacteria attaching to particular surfaces are responsible for the biofilm formation.

A surface-associated bacteria was first observed by Anthony van Leeuvenhoek even though the term 'biofilm' was not coined. In 1999, it was Costerton et al. who gave a definition for biofilm as 'a structured community of bacterial cells enclosed in a self-produced polymeric matrix, adherent to a surface'. Since then, biofilm is considered as a serious issue and it is a challenge to eradicate them. Biofilm formation of two bacterial strains is shown in figure 1.1.

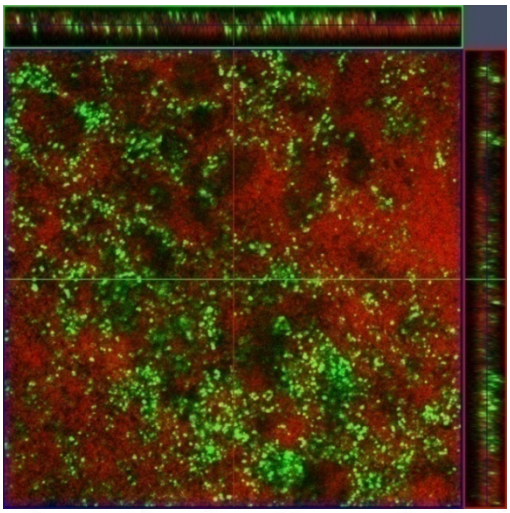

Figure 1.1 Biofilm formed by *Pseudomonas Aeruginosa* (Red) and *Staphylococcus epidermidis* (Green) (Armijo et al., 2020)

The biofilm components can be categorized into six : polysaccharides, proteins, nucleic acids, lipids, water and ions like Ca^{2+}, Mg^{2+}, Cl^{-}, PO_4^{2-}(Joshi *et al*., 2020). This composition may vary in accordance with the species of bacteria, surrounding environment and availability of nutrients.

1.2.1 Bacterial adhesion and biofilm formation

Several sequential steps are involved in biofilm formation. Initially, planktonic bacteria stick to a solid surface. It is followed by cell proliferation, cell-cell interaction and production of extracellular matrix. After the initial attachment bacteria will start growing and colonization takes place. Based on intercellular adhesion and bacterial attachment, multicellular clusters are formed. Exopolysaccharides, proteinaceous factors, extracellular DNA and enzymes are responsible for inducing this step. When this structure is fully developed and matured, some bacteria detach and disperse into the surrounding. This cause biofilm to spread everywhere. Detailed steps involved in biofilm formation are shown in figure 1.2.

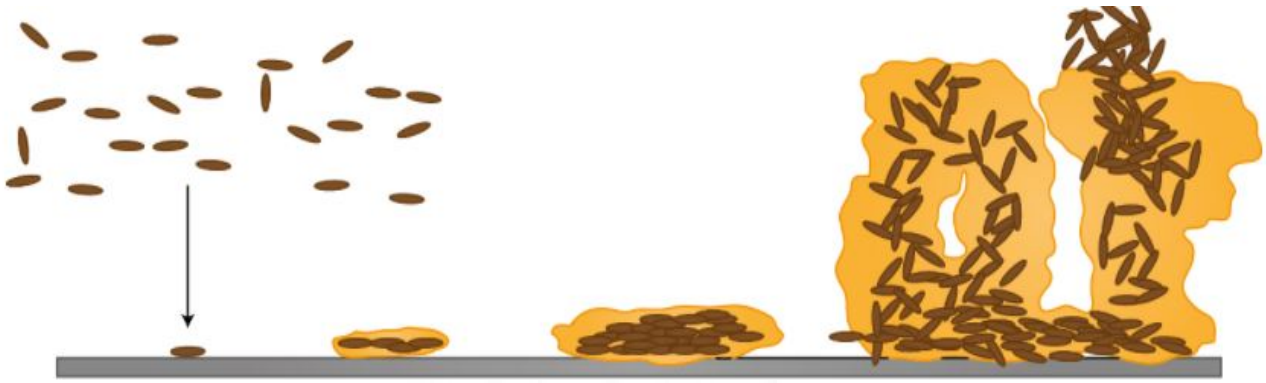

Figure 1.2 Schematic representation of biofilm formation (Trafny; 2008)

i. Attachment - Bacteria is adhered to the surface. The molecular signalling systems equipped by the bacteria are used in a process called quorum sensing. With an enough number of cells, the signalling may reach a threshold value and it triggers several other mechanisms like gene regulation. It is mediated by its surface modifications like flagella, pili etc. The attachment is irreversible through the production of extracellular matrix. When bacteria is attached to a surface, it results in the alteration in the expression of a number of genes responsible for exopolysaccharide production (Khatoon *et al*; 2018).

ii. Formation of microcolony – After the formation of colony, motility factor is inhibited and multilayers are formed later.

iii. Formation of matrix – The cell-cell communication such as quorum sensing and extracellular polymeric substances (EPS) helps for the maturation of biofilm. Due to polysaccharides, characteristic "mushroom" like structures are developed. The exopolysaccharide matrix is a protective barrier for bacteria against the antibiotics.

iv. Dispersal of cells – Mature biofilm releases a secondary messenger molecule. It helps in the dispersal of biofilm matrix and the cells are again in planktonic state to repeat the entire process (Trafny; 2008).

1.2.2 Biofilm and its threats

After the biofilm formation, the bacteria can transfer genetic material like antibiotic resistant genes among themselves. In this way, bacteria limit the action of treatments. The bacteria detached from the biofilm community may settle somewhere else in the body and create other sources of infection. This type of bacterial organization is responsible for the large number of chronic infectious diseases.

Moreover, biofilm formation is one of the major challenges faced in patients with indwelling or long duration implanted medical devices. Commonly, different parts of medical devices are made of different materials. These transition zones of materials provide excellent opportunity for the bacteria to adhere and form biofilm. Orthopaedic, dental and cardiovascular implants are the main mixed-surface devices (Gomes & Mergulhão, 2017). In medical devices, both gram-positive and gram-negative bacteria can form biofilms. For example, *Pseudomonas aeruginosa*, which belongs to ESKAPE pathogens (a group consisting of ***E****nterococcus faecium,* ***S****taphylococcus aureus,* ***K****lebsiella pneumoniae,* ***A****cinetobacter baumannii,* ***P****seudomonas aeruginosa,* and***E****nterobacter species*), is a gram-negative bacterium, which shows high resistance to a range of antibiotics (Armijo *et al*., 2020). Formation of biofilm leads to prosthetic heart valve infections, catheter biofilm infections, blood stream infections. 80% of chronic infections and 60% of infections acquired in health care facility are due to biofilm formation. The type of infections such as in the case of endocarditis, pneumopathies, skin wounds contribute significantly to nosocomial infections. ESKAPE bacteria play a major role in causing majority of such nosocomial infections.

The biofilm EPS layer exhibits strong resistance against human immune system and prevent antibiotic drugs to penetrate. This barrier is a limitation for the treatment even for antibiotic-susceptible strains. Especially in the case of CF respiratory tract infections, the drug has to penetrate two barriers; the EPS layer of biofilm and the thick CF mucus layer. In such conditions, the antibiotic drugs do not serve the desired function. To overcome the limitations of antibiotic treatment for microbial infections, nanomaterials are widely used. These inorganic materials do not allow microbes to develop resistance against them. The nanomaterials show same antimicrobial activity even after multiple uses (Vallabani & Singh, 2018). Thus, the limitations of conventional drugs lead to the development of nanoparticles having versatile properties including antibacterial effects.

1.3 Nanoparticles as antimicrobial agents

Several types of nanoparticles have been proved as effective agents in killing bacteria and eradicating biofilm. Nanoparticles with antimicrobial properties can be classified into metallic nanoparticles, polymeric nanoparticles, carbon-based nanoparticles, lipidic nanoparticles, non-metallic nanoparticles etc. Among these, various metal and metal oxide nanoparticles are found to be more efficient as antibacterial agents. Because of their physicochemical characteristics, such as surface charge, hydrophobicity and high surface area ratio by volume, nanoparticles can adsorb and penetrate into biofilms. Metal oxide nanoparticles have so many advantages compared to nanoparticles of other categories. Some of them are capable of bringing structural changes that can alter the cell parameters and lattice symmetry, change in the electrochemical properties due to the quantum confinement and variation in surface properties which can lead to an increase in the band gap of the material. This property influences the conductivity and other chemical properties of nanomaterials (S.Immanuel *et al.,* 2019). Another important specialty of metal oxide nanoparticles

is their biocompatibility towards the immobilization of enzymes, which helps in the efficient sensing of biomolecules.

Depending on their size, shape and the surface properties, metal oxide nanoparticles act on the systems differently. The size influences the surface area to volume ratio of these materials which affect the material uptake and biodistribution of nanoparticles. So it is essential to have a better understanding on the morphology of the synthesizing nanoparticle. Metal oxide nanoparticles can be classified into zero-dimensional, one-dimensional, two-dimensional and three-dimensional nanoparticles, depending on their confinement (Nikolova *et al*., 2020). Thus the properties of metal oxide nanoparticles vary according to their size and shape for various applications such as drug delivery, biosensors, antimicrobial agents, immunotherapy etc.

As an antibacterial agent, metal oxide nanoparticles are promising candidates since antibiotic (AB)-resistant pathogens are very common. It is due to the transfer of AB resistance genes between bacteria, there is growing concern over the effect of existing antibiotics. Most of the metal oxide nanoparticles impart their antibacterial mechanism through ROS generation or by releasing metal ions. These nanoparticles can cause depletion in the ATP production and DNA replication. A wide range of metal oxide nanoparticles such as Titanium oxide, Aluminium oxide, Magnesium oxide, Calciumoxide, Silver oxide, Iron oxide etc are found to have antibacterial properties. Also Nickel oxide nanoparticles exhibit bactericidal and bacteriostatic activity depending on the bacterial strain and bacterial concentration. While combining silver (Ag) nanoparticles with other nanoparticles, it has been found out that, the combination has produced a synergetic antibacterial effect (G.Devi *et al*., 2014). But studies have shown that, besides these antibacterial properties, most of these metallic nanoparticles show significant levels of toxicity. For example, Ag nanoparticles can get absorbed through the lungs, skin and intestine into

circulation. Nano-silver can penetrate into the cells and cause cellular damage. The exposure and accumulation of TiO_2 in lungs can cause inflammation and bleeding. In this context, magnetic nanoparticles offer versatile applications.

1.3.1 Iron oxide nanoparticles

Iron oxide nanoparticles (IONPs) have excellent nanoscale physical properties such as superparamagnetism, biocompatibility and chemical stability. Due to these properties, they are extensively used in biomedical applications especially in biomedicine, biosensor, magnetic resonance imaging, targeted drug delivery, hyperthermia etc. Iron oxide nanoparticles are biologically inert. IONPs especially, Fe_3O_4 nanoparticles are distinct from other nanoparticles because of the combination of Fe^{2+} and Fe^{3+}ions. Fe^{2+} ions are arranged in the octahedral sites and Fe^{3+}ions are organized across octahedral and tetrahedral sites. IONPs are potential candidates for both biological and technical applications due to their feasible polymorphism and electron hopping nature (Vallabani & Singh, 2018). IONPs having size about 10-20 nm are said to be superparamagnetic IONPs (SPIONs). The schematic representation of SPIONs showing the core radius and the hydrodynamic radius is depicted in figure 1.3.

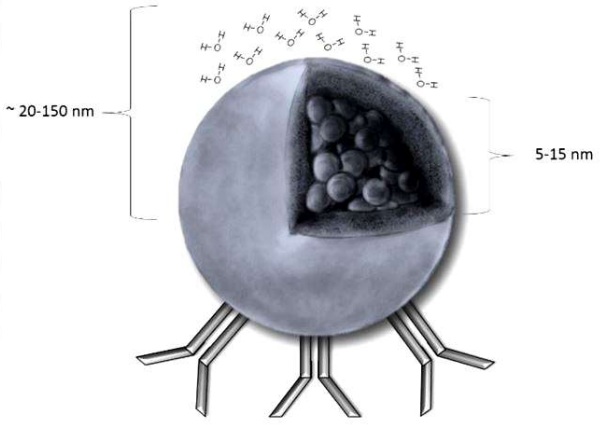

Figure 1.3. The schematic representation of SPIONs (Dulińska-Litewka et al., 2019)

SPIONs are being developed as a contrast agent for MRI. The unique magnetic properties and the capability to function on cellular and molecular level make these nanoparticles an effective candidate for MRI applications. The magnetic properties and enzyme like activity of IONPs for various biomedical applications is shown in figure 1.4.

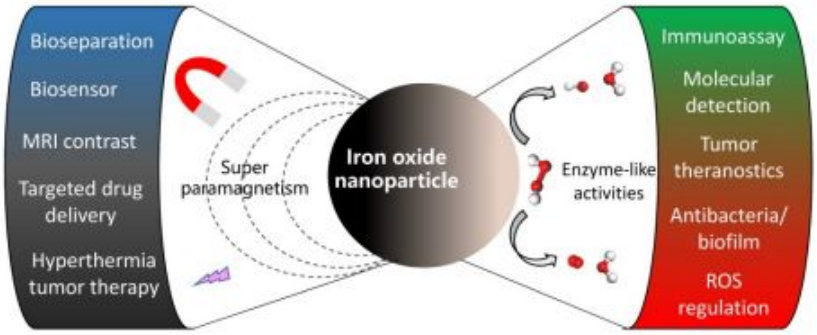

Figure 1.4. Magnetic properties and enzyme-like characteristics of IONPs (Gao L *et al.*; 2017)

Above all these, IONPs show intrinsic enzyme-like activity. Thus these nanoparticles can be termed as iron oxide nanozyme (IONzyme). In association with hydrogen peroxide (H_2O_2), these nanozymes shows enhanced antibacterial effect on bacterial biofilms compared to the nanozymes without H_2O_2 (Gao *et al.*;2016). The mechanism involving the generation of cell toxicity is depicted in Figure 1.5. IONzyme is reported to have two enzymatic activities; peroxidise and catalase. Porphyrin heme is present as cofactor in the active sites of these two enzymes and H_2O_2 is used as the substrate by both.Peroxidase activity is seen in both Fe_2O_3 and Fe_3O_4 nanomaterials. Since Fe_3O_4 nanoparticles have both Fe^{2+} and Fe^{3+} ions, the transitions of these ions at octahedral sites result in the heterogeneous Fenton reaction. Fe_3O_4 nanoparticles follow the heterogeneous Fenton reaction by generating ˙OH radicals from surface $Fe^{2+}$and H_2O_2. In homogeneous Fenton reaction, Fe^{2+} ions react with H_2O_2 to generate ˙OH radicals. Free radicals (˙OH) are generated in this process only. Fenton reaction is depicted in equation 1. They react

with free radicals. The concentration of H_2O_2 should be maintained in an optimum value for the peroxidise activity (Gao L *et al.*; 2017).

$$Fe^{2+} + H^+ + H_2O_2 \rightarrow Fe^{3+} + {}^{\bullet}OH + H_2O_2 \qquad \textbf{(1)}$$

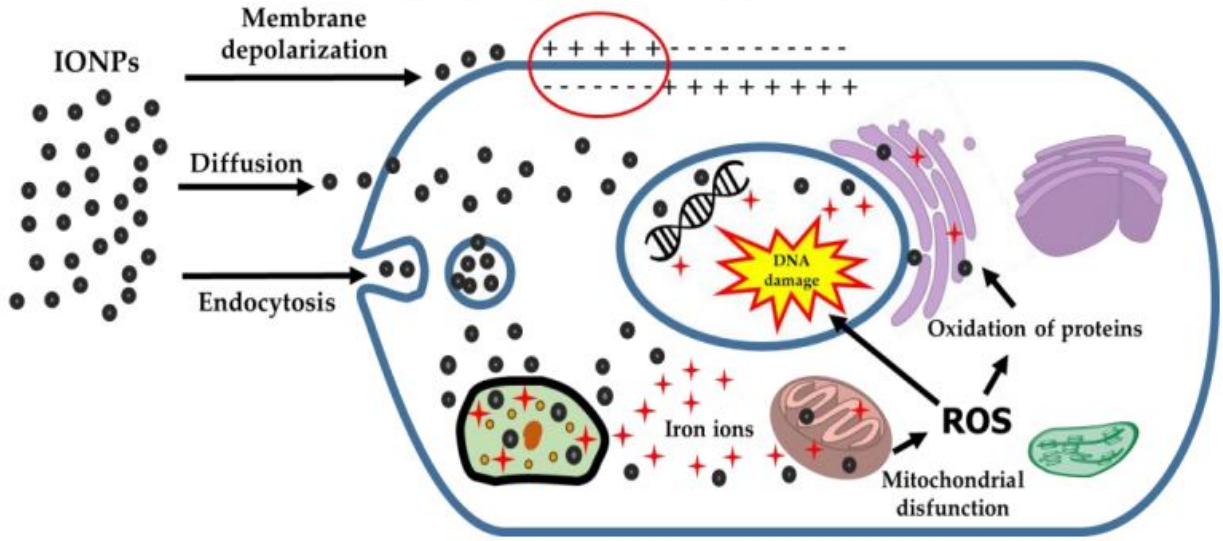

Figure1.5. Different mechanisms of generating cell toxicity by iron oxide nanoparticles (Arias, L. S. *et al.*2018)

Compared with other enzyme mimetics and natural enzymes, these nanozymes possess some other properties like high stability, tunability and multifunctionality. In extreme conditions like high temperature, acidic or basic conditions, IONzymes show excellent stability.

1.3.2 Antibacterial properties and biofilm elimination

Ironoxide nanoparticles exhibit antimicrobial activity through various mechanisms such as membrane depolarization, production of ROS and releasing of metal ions (Arias, L. S. *et al.;* 2018). Membrane depolarization causes impairment of cell integrity. IONPs enter the bacterial

cell through diffusion. Upon reaction with H_2O_2, Iron oxide nanoparticles generate free radicals. These free radicals are highly toxic and they can attach the cell membrane and nucleic acids and it leads to the malfunctioning of bacteria. IONPs can also enter inside the cell by endocytosis. After entering metal ions are released into the cytoplasm and it affects the cellular homeostatsis and protein coordination.

1.3.3 Effect of coating on IONPs

Several studies have been done regarding the toxicity of IONPs. Size and shape of nanoparticles also influence the toxicity levels of these nanoparticles.Researchers have shown that rod-shaped IONPs are more toxic than their spherical counterparts. The production of ROS may cause cellular oxidative stress. IONPs have the tendency to accumulate in the lysosomes and they are degraded in iron ions. The ions crossing the membrane can reach the organelles such as nucleus and mitochondria and react with H_2O_2. This leads to the generation of ROS. Uncoated IONPs are found to have disturbed the cell membrane functions. This eventually leads to leakage of lactase dehydrogenase and bubble-like extensions in the cell body. Also IONPs are very prone to aggregation after long-term storage and have a tendency to lose magnetic properties due to the oxidation in air. So it is essential to implement desirable methods to stabilize the nanoparticles.

To make IONPs less toxic and to improve biocompatibility, surface modifications can be done. Coating decreases the oxidative sites and hence less DNA damage occurs. Different types of coating can be employed inorder to make IONPs non-toxic. Core-shell nano structures are more preferred to attach the drugs in IONPs. Polymers, organic surfactants, inorganic compounds, bioactive molecules etc can serve as shell structure. Such coatings can also increase non-specific intracellular absorption.

1.4 Poly-L-Lysine (PLL)

PLL ($(C_6H_{12}N_2O)_n$) is a cationic polymer, which is water soluble. The structure of PLL is shown in Figure 1.6. The monomeric unit of PLL is L-lysine, which is one of the 20 naturally occurring amino acids. For both eukaryotes and prokaryotes, this amino acid is essential for protein functions and injury recovery.

Because of the protonation of primary amino groups, these polymers are positively charged. Due to this cationic property and its inherent properties like biocompatibility, biodegradability and non-antigenicity, PLL has a wide range of applications in biomedical field. PLL is being widely used as nano carriers, coating materials, biofilm dispersal agent etc (M. Zheng et al;2021). Moreover, the side chains of these polymers can be modified and coupled to any therapeutic drugs. For these reasons, PLL is suitable candidate for designing therapeutic agents.

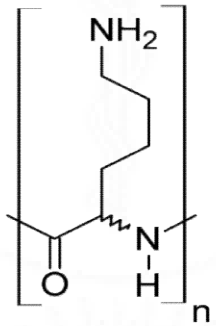

Figure 1.6. Structure of Poly-L- Lysine

1.4.1 PLL as antibacterial agent

Bacterial infection is a major threat across the world. Eventhough antibiotics are readily available, they are not complete solution for such infections. Bacteria that form biofilms show strong resistance towards these antibiotics. In this context different types of antibacterial materials

are synthesized to attack the drug-resistant pathogens. Antimicrobial peptides (AMPs) are one of such antibacterial agents which kills the bacteria by disrupting the bacterial cell membrane. AMPs are composed of basic aminoacids such as lysine and arginine and has positive charge. Because of this cationic charge, AMP can combine with negative charges on the surface of gram-positive (cell wall) and gram-negative (outer cell membrane) bacteria via electrostatic interaction, resulting the destruction of bacteria.

PLL based polymers have gained attention nowadays since they are inspired from the structure of AMPs and has wide range of uses such as antibacterial materials mimicking AMPs, antibacterial coatings, and antibacterial hydrogels. PLL also attaches to bacterial membrane by electrostatic attraction since it has a high concentration of positive charges due to the presence of amino groups.

1.5 Hypothesis

Several antibiotics are available to treat the biofilm related infections. But almost all pathogenic bacteria show resistance to these antibiotics. Eventhough many nanoparticle based antibiofilm agents, mostly silver nanoparticles, are studied extensively, they all imparts some level of toxicity. Antimicrobial properties of iron oxide nanoparticles have been extensively studied. It has been proved that iron oxide nanoparticles alone could not disrupt the bacterial biofilm. By considering these facts, it is hypothesized as,

i. Surface modification of uncoated SPIONs with a biocompatible polymer will decrease the toxicity.
ii. The coating with an appropriate polymer will enhance the antibacterial property of iron oxide nanoparticles and leads to the complete destruction of bacterial biofilm.

1.6 Objectives of the study

Based on the above hypothesis, the objectives of the proposed study are,

- To synthesize super paramagnetic iron oxide nanoparticles (SPIONs) via co-precipitation method.
- Modify the SPIONs with a biocompatible polymer with antibacterial properties.
- To study the effect of synthesized polymer coated nanoparticles in prevention and destruction of biofilm formed by both gram-negative and gram-positive bacteria.

CHAPTER 2

REVIEW OF LITERATURE

2.1 Nanoparticles as antimicrobial agents

Nanoparticles, especially metal-based nanoparticles have gained wide popularity for their efficiency and versatile action as antimicrobial agents. There are a number of metal-based nanoparticles, which offers several biomedical applications. Raghunath *et al*. have synthesized and characterized Aluminium oxide (Al_2O_3) nanoparticles and studied their effect on the clinical isolates of *E.Coli.* The nanoparticles inhibited the growth and multiplication of the bacteria. (Raghunath *et al*.,2017). Similarly, numerous metal-based nanoparticles such as Antimony trioxide (Sb_2O_3) NPs, Chromium oxide (Cr_2O_3) NPs, Cobalt oxide (Co_3O_4) NPs, Magnetite (Fe_3O_4) NPs, Zinc Oxide (ZnO) NPs etc have been established as promising antibacterial agents (Rakesh *et al*., 2013; Gosh *et al*.,2014; Agarwala *et al*., 2014).

Most commonly exploited metal-based nanoparticles for medical and pharmaceutical applications are Silver (Ag) NPs, gold (Au) NPs, Zinc oxide (ZnO) NPs, Copper oxide (CuO) NPs and Magnetite (Fe3O4) NPs. It has been reported that, among metal-based nanoparticles, Ag NPs showed good efficiency as antibacterial agent. But, their accumulation inside the body can cause severe toxicity (Paladini & Pollini, 2019; Lopez *et al*., 2020; Szerencsés *et al*., 2020). Likewise, there are reports that, Au NPs which were administered orally in rats caused decreased body weight and red blood cells (Zhang *et al*., 2010). Au NPs were primarily investigated for imaging applications and not as an antimicrobial agent. Since these nanoparticles are relatively inert and biocompatible, their antimicrobial properties are being vastly studied. Compared to Ag NPs, Au NPs showed less antimicrobial activity (Asharani *et al*., 2011). In this context, magnetic

nanoparticles are creating a significant progress on diagnosis or nanomedicine or a combined platform of both called theranostics (Veera *et al*., 2019).

2.1.1 Iron oxide nanoparticles

Among metal nanoparticles, iron oxide nanoparticles (IONPs) are one of the mostly studied particles. For the macroscopic applications, iron's reactivity plays an important role. Finely divided iron is also found to be pyrophoric. (Ali *et al*., 2016). Due to these reasons the potential applications of iron was not widely explored. The past few decades witnessed a drastic development in the field of nanotechnology, especially the applications of magnetic nanoparticles. Iron oxide nanoparticles have drawn attention due to their excellent magnetic such as superparamagnetism, antibacterial and enzymatic properties as well as their well established fenton chemistry and high stability. Major works reported regarding the applications of IONPs include maghemite (γ-Fe_2O_3) or magnetite (Fe_3O_4). Magnetite nanoparticles are the mostly studied nanoparticles among these because of its biocompatibility (Mahmoudi *et al*., 2011). In 2007, intrinsic peroxidase-like activity was discovered for ferromagnetic (Fe_3O_4) nanoparticles. It was for the first time an inorganic nanoparticle was recognized as an enzyme mimetic.

Recently, several studies have carried out to investigate the unique enzymatic properties of magnetite nanoparticles (Gao *et al*., 2017). Gao *et al*; in their work, has reviewed the enzymatic properties of IONPs, termed as nanozyme and summarized its novel biomedical applications. Several works have done to investigate the effect of buffers, pH and presence of ATP on the peroxidase activity of magnetite nanoparticles (Vallabani *et al*., 2017, 2019). Vallabani *et al*. explained that, from the synergistic combination of Fe_3O_4 nanoparticles and nucleotides, hydroxyl (OH) free radicals were generated and it resulted in an enhanced peroxidase activity at neutral pH.

Also it was found out that, the peroxidase activity is strongly affected by buffer conditions. The enzyme-mimetic properties can be utilized for the development of non-enzymatic biosensors which is used to test the concentrations of glucose, gluthione cholestrol, H_2O_2 etc (Gawande *et al*., 2016, Wang *et al*., 2017). Gawande *et al*. have shown that these biomolecules are biomarkers for several diseases and the biosensors thus developed can be used for the early diagnosis of diseases like cancer. To improve the catalytic activity of nanozymes, Yu *et al*. have studied the significance of citrate, heparin, dextran and polylysine coating on magnetic nanoparticles (Yu *et al*., 2009). It was observed that the nanoparticles with positive charge showed high affinity towards 3,3',5,5'-tetramethylbenzidine (TMB), which is a substrate involved in glucose detection.

IONPs have also found applications in antibacterial and antifungal studies. There are reports regarding the inhibitory effect of Fe_3O_4 nanoparticles on *Escherichia coli, Bacillus subtilis, Candida albicans, Aspergillus niger and Fusarium solani*(Arakha *et al*., 2015). Patra *et al*. have synthesized Fe_3O_4 nanoparticles from corn plant extract and showed that these nanoparticles have antibacterial and anticandidal activity (Patra *et al*., 2017). Gao *et al*. also did a similar work where they synthesized Fe_3O_4 nanoparticles from *Couroupita guianensis* fruit extract and observed that the synthesized nanoparticles have strong antibactericidal action on several human pathogens (Gao *et al*., 2017).

Hussein-Al-Ali *et al*. prepared a nanosystem combining IONPs, chitosan (CS) and Nystatin (NYS) (Hussein-Al-Ali *et al*., 2015). The IONPs-CS-NYS nanosytem showed a release profile of 1800 minutes, while the most common fungicide NYS can last about 20 minutes only. From majority of the works it is clear that, bare IONPs alone could not provide all the desirable actions *in vivo* including biocomptibility and non-toxicity. To improve the colloidal stability of iron oxide nanoparticles, Yang *et al*. coated Fe_3O_4 nanoparticles with polyacrylic acid (PAA),

poly(vinyl alcohol) (PVA) and polyethyleneimine (PEI) (Yang *et al.,*2017).They observed that, polymer coated Fe_3O_4 nanoparticles showed higher stability and dispersivity. PEI coated Fe_3O_4 was found to show high toxicity than any other coatings. Some of the polymer coatings employed on iron oxide nanoparticles are summarized in Table 1.

Polymer coating used on SPIONs	References
Polyacrylic acid (PAA)	Yang *et al.,* 2017
Polyvinyl Alcohol (PVA)	Sakulku *et al.,*2014 Yang *et al.,* 2017
Poly(isobutylene-alt-maleic anhydride) (PMA)	Ahmadpoor *et al*., 2021
Polypyrrole (PPy)	J Anitta *et al*., 2021
Dextran	Sakulku *et al.,*2014
Polyethylenimine Polyethylene glycol	Barrow *et al*., 2015

Table 1. Polymer coatings on SPIONs

Thus it is understood that, coating of IONPs is essential inorder to increase the action without toxic effects. Researchers have modified SPIONs with a variety of polymers for various applications. Poly-L-lysine is also a kind of polymer which is biocompatible and has several advantages. Studies showing PLL modified SPIONs are not much reported.

2.2 Poly-L-lysine (PLL)

Poly-L-lysine is a cationic, biocompatible polymer which consists of monomeric units of α-lysine. PLL exhibits good water solubility and hence they are hydrophilic. Several studies have conducted to explore the versatile properties of PLL for various biomedical applications. Since

high-molecular weight PLLs are considered as toxic than their low-molecular weight counterparts, researchers have been trying for the structural modification of PLL to alleviate their toxicity (Zheng *et al*., 2021). Such modifications could improve the structural affinity of PLLs towards bacterial effect and enhance the the antibacterial activity.

PLL has been proved as an effective candidate in counteracting microbial contamination and biofilm-infected medical implants (Schilardi *et al*., 2018). Schilardi *et al* had used PLL as a mediator for applying silver nanoparticles on the titanium surfaces. They have reported an enhanced antibacterial efficacy of silver nanoparticles compared to those which are not functionalized with PLL. Ma *et al*. in their work have reported the antimicrobial and antifouling polymer brush coatings, which exhibited antimicrobial efficacy against the pathogens like *S.aureas, E.Coli, P.aeruginosa and Candida albicans.* Kang *et al*. have functionalized tannic acid with PLL which are self-assembled through coordination chelation with stainless steel. These stainless steel surfaces exhibited good resistance to bacterial adhesion and microalgal attachment. Hyldgaard *et al*. have examined the effect of PLL on cell morphology and membrane integrity of*Escherichia coli* and *Listeria innocua*. It was seen that, PLL has successfully removed the lipopolysaccharide layer and the cell morphology of *E.coli* was affected(Hyldgaard *et al*., 2014). In a similar work, Wei *et al*. have studied the antimicrobial property of ε-PL against *Pseudomonas aeruginosa* and *Aspergillus fumigatus*(Wei *et al*., 2017). It has been reported that PLL based multilayer films are inherently antibacterial without any covalent modifications or addition of other antibacterial substances. Eventhough the PLL films are of different molecular weight, it was seen that all of them have completety inhibited the bacterial growth (Alkekhia & Shukla, 2019).

Durmus *et al*. have synthesized and characterized L-lysine coated iron oxide nanoparticles. (Durmus *et al*., 2009; Yang *et al*., 2015). Yang *et al*. have prepared PEG coated SPIONs and then

it was modified by PLL. Several works have reported the ability of PLL in *in vivo* tracking studies. To evaluate the cellular uptake of neural stem cells, Pongrac . have prepared and characterized PLL-coated maghemite nanoparticles and compared them with the commercially available dextran-coated SPIONs (Pongrac *et al*., 2016). The results showed that, the biocompatibility and cell-labelling efficiency of maghemite nanoparticles have improved upon coating with PLL.

2.3 Biofilm formation and anti-biofilm strategies

Each year, tens of millions of medical devices are used for various purposes. Eventhough many advances have made in biomaterials, majority of medical implants are facing the threat of bacterial colonization and thus implant-related infections are emerging. After the formation of biofilm, the biofilm bacteria show 10 to 10,000 times higher resistance towards antibiotics than their counterparts in planktonic state (Tierlinck *et al*.; 2017).In recent years, synthesis of anti-infective biomaterials is a growing area to counteract such biomaterial associated infections. Several approaches can be employed to develop novel anti-biofilm strategies (Paunova-Krasteva *et al*., 2020). Some of them are synthesizing antiadhesive surfaces that can be applied on to the medical devices and developing a method to destroy the pre-formed bacterial biofilm. Paunova-Krasteva *et al*. in their work employed the latter strategy by developing a cationic polymer micelle bearing silver nanoparticles to destroy the biofilm formed by the bacteria *Pseudomonas aeruginosa*. These micelles were successful candidates for the eradication of the bacterial biofilm.

Application of metals in nanolevel is considered as an excellent choice to resolve the biofilm formation. Nanocomposites of metal oxides are also developed to enhance the antimicrobial properties and reduce the cytotoxic effects. Various metal nanoparticles like silver

and iron, are widely used because of their antibacterial properties (Guo *et al*., 2019). Guo *et al*. studied the role of concentration of silver nanoparticles on biofilm degradation. Antimicrobial properties of silver and the dependence of their size has been studied in detail which find its application in woundhealing and biofilm preventive agents (Paladini & Pollini, 2019; Szerencsés *et al*., 2020). The major concern in all these works was the toxic effects of Ag nanoparticles. As explained above, eventhough many nanoparticles have been explores as excellent antimicrobial agents, their accumulation and interaction can create toxic effects in living systems. Ravichandran *et al.* have shown that, the toxicity of ZnO nanoparticles can be greatly reduced through doping with iron (Ravichandran *et al*., 2015). Similarly, ZnO nanoparticles doped with Fe and Mn also showed improved antibacterial activity against a wide range of bacteria including *S. aureus, E. coli, K. pneumoniae, S. typhi, P. aeruginosa, B. subtilis,* and *Proteus mirabilis.* The mechanism of interaction of nanoparticles on biofilm is through three stages (Figure 2.1).

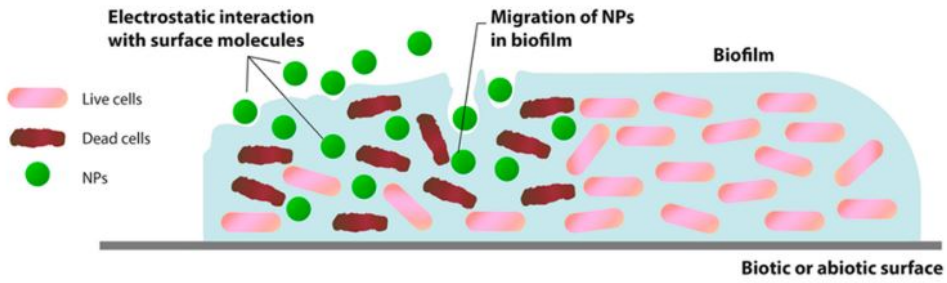

Figure 2.1. Interaction of nanoparticles with biofilm (Shkodenko *et al*., 2020)

The transfer of nanoparticles, attachment of nanoparticles on the surface and migration into the biofilm (Shkodenko *et al*., 2020). The progression of each and every stage depends on the surroundings and the properties of nanoparticles.

Among all other metal-based nanoparticles, magnetic nanoparticles are somewhat superior due to their magnetic properties. In the presence of magnetic field, these nanoparticles can

penetrate deep into the biofilm in addition to its passive electrostatic effect on biofilm. The nanoparticles impose a mechanical effect by destructing the matrix structure and the whole architecture of the bacterial biofilm. The mechanisms responsible for the antimicrobial effects of nanoparticles is depicted in figure 2.2.

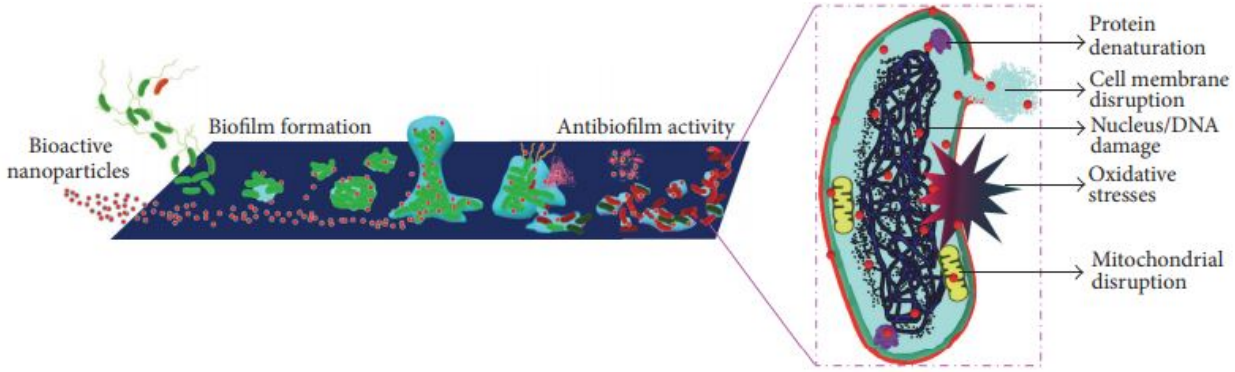

Figure 2.2. Mechanisms responsible for the antimicrobial action of NPs (M Ramasamy *et al*., 2016)

Recently many studies have highlighted the importance of magnetite (Fe_3O_4) nanoparticles as an effective matrix for delivering biocides inside the biofilm (Wilczewska *et al*., 2016). Thukkaram *et al*. have investigated the effect of iron-oxide nanoparticles over biofilm formation on pluronic coated surfaces and different biomaterial surfaces(Thukkaram *et al*., 2014). Compared to other surfaces, a significant reduction in biofilm growth was observed in the presence of the highest concentration of iron-oxide nanoparticles on pluronic coated surfaces. Sathyanarayanan *et al*. have demonstrated the role of gold and iron oxide nanoparticles on the destruction of biofilm produced by *Staphylococcus aureus* and *Pseudomonas aeruginosa*(Sathyanarayanan *et al*., 2013). Reports show that surface modified magnetic nanoparticles can be effective nanomaterials for antibacterial treatments.

CHAPTER 3

MATERIALS AND METHODS

This chapter deals with the materials and methods used for the synthesis, characterization and the antibacterial studies of the uncoated and coated SPIONs. The details on the synthesis of the nanoparticles and characterization techniques used to evaluate the structural properties of the synthesized materials such as shape, size, surface charge are described. This chapter also deals with various *in vitro* techniques to understand the antibacterial properties of the synthesized material.

3.1 Materials

The chemicals employed for the study are either purchased or freshly prepared. Distilled water was used throughout the study. Ferrous chloride and Poly-L-lysine (Molecular weight: 3000 to 7000 Da) were purchased from Sigma Aldrich, USA, Ferric chloride from Ranbaxy and Sodium hydroxide pellets from EMPLURA®. For cell culture studies, fetal bovine serum, trypsin, EDTA and MTT reagentwere obtained from HiMedia, India. MEM and streptomycin were from Gibco, USA.

3.2 Methods adopted

3.2.1 Synthesis of Super paramagnetic Iron oxide nanoparticles (SPIONs)

Ferric chloride ($FeCl_3$) and Ferrous chloride ($FeCl_2$) are used as starting reagents. The synthesis was done via co-precipitation technique. 4.06g $FeCl_3$ and 1.59g $FeCl_2$ was mixed with 50ml distilled water with vigorous magnetic stirring for 60 minutes. The solution was heated at

30ºC in a three-neck round bottom flask under the constant flow of nitrogen. To the solution, 30 ml freshly prepared sodium hydroxide (NaOH) solution (2M, 8g/100ml) was added drop by drop.

A black precipitate was formed indicating the formation of iron oxide nanoparticles (Equation 2). For the washing purpose, 82.84 ml distilled water and 17.16 ml hydrochloric acid was added to the precipitate formed. The solution was centrifuged at 8000 rpm for 20 minutes. Then the supernatant was separated and repeatedly washed with distilled water and hydrochloric acid (HCl).

$$Fe^{2+} + 2Fe^{3+} + 8OH^- \rightarrow Fe_3O_4 + 4H_2O \quad \textbf{(2)}$$

3.2.2 Synthesis of Poly-L-Lysine (PLL) modified iron oxide nanoparticles

Iron oxide nanoparticles were taken at different concentrations (25µl, 50µl, 100µl, 150µl and 200µl as Sample 1, Sample 2, Sample 3, Sample 4 and Sample 5 respectively). To each sample, freshly prepared PLL solution (1mg/ml) was added. The samples were placed in vortex machine for 20 minutes, followed by ultrasonication for 10 minutes. Centrifugation was done at 1000 rpm for 20 minutes. The supernatant was removed and the samples were stored at -80ºC for 24 hours for lyophilisation.

3.2.3 Characterization of nanoparticles

3.2.3.1 X-ray diffraction technique (XRD)

X-ray diffraction technique was carried out using Bruker D8 ADVANCE with DAVINCI design, to analyse the phase of the synthesized SPIONs in powder form. To understand the crystal structure, the position and intensities of diffraction peaks were observed in the range of diffraction angle $2\theta = 5^{\circ}$ to 90°. Cu Kα radiation of 1.5406 Å at 40kW and 40 mA was used for the analysis.

The XRD patterns wereanalyzed by quantitative Rietveld pattern refinement using the Topas software (4.2).

3.2.3.2 Transmission Electron Microscopy (TEM)

The size and morphology of the synthesized nanoparticles were examined using transmission electron microscopy. The particles separated using centrifugation were thoroughly washed and dispersed in distilled water. Small amounts of dispersed samples were dropped on a copper grid for TEM observation and allowed to dry.

3.2.3.3 Dynamic Light Scattering technique (DLS)

Zeta potential measurements and hydrodynamic diameter of the prepared nanoparticles were analysed using dynamic light scattering instrument (DLS, Zetasizer NanoZS90, Malvern instruments Ltd:, Worcestershire, UK). Very small amounts of samples were dispersed in distilled water at very low concentration, followed by ultrasonification for 20 minutes. The instrument consisted of a He-Ne laser where the solution is placed. All the measurements were taken at 25ºC, which is the standard temperature of the instrument.

3.2.3.4 Fourier Transform Infrared Spectroscopy (FTIR)

FTIR spectra of PLL coated and uncoated SPIONs were taken usingAgilent Cary 660 FTIR spectrometer. The samples in the form of powder, prepared by freeze-drying, were grounded with KBr and compressed into a pellet. The IR spectra were recorded in the range of 4000 - 400 cm^{-1} to understand the type of chemical bonds formed.

3.3 Cell culture studies

Cell culture studies were performed using mouse fibroblast cell line (L-929, American Type Cell Cultures, USA). Cells were cultured in Minimum Essential Medium (MEM: Gibco, USA) containing 5% fetal bovine serum (South American Origin, HiMedia, India) and 100 IU/mL penicillin and 100 µg/mL streptomycin (Gibco, USA) in a CO2 incubator (New Brunswick, Eppendorf India), set at 37ºC, 5% CO2 and 95% relative humidity. Confluent cells were harvested using Trypsin (0.25%) –EDTA (0.02%) and 5×10^4 cells were seeded to 96 well plates.

3.3.1 Cytotoxicity assessment

Different dilutions of uncoated and PLL-coated SPIONs (200, 100, 50, 25 and 12.5 µg/ml) were prepared in the culture medium. Culture medium of cells in 96 well plate was replaced with l00µl test sample medium and incubated in CO_2 incubator for 24 hours. After the removal of test sample medium, the cells were treated with 50µl MTT reagent (0.5 mg/ml inµcells were treated with 50°C. serum free medium) and incubated for 2 hours at 37ºC. The cell morphology was investigated using inverted phase contrast microscope (Nikon TS100, Japan). The formazan product formed was solubilized in isopropanol and absorbance was taken at 570 nm in a plate photometer (Biotek Powerwave XS, USA). The percentage viability was calculated using the relation :

$$Percentage\ cell\ activity = \frac{Absorbance\ of\ test}{Absorbance\ of\ control} \times 100 \qquad \textbf{(3)}$$

3.3.2. ROS Assay

The test samples were in the form of suspension in distilled water with concentration 1mg/ml. Reactive oxygen species (ROS) generated in cells subsequent to exposure of L-929 cells to uncoated SPIONs and PLL-coated SPIONs was measured using cell-permeant 2',7'-dichlorodihydrofluorescein diacetate (H2DCFDA) assay. Cell monolayer on 12 well plate was exposed to uncoated SPIONs (200 µg/ml) and PLL-coated SPIONs (200 µg/ml); both at non-cytotoxic dose. Culture medium from cells were replaced with 100µl test sample (uncoated SPIONs and PLL-SPIONs, n=4) medium and incubated in CO_2 incubator for 24 hours. Cell exposed to normal culture medium was considered as control.

Test sample medium was removed and cells were treated with 500 µl cell-permeant 2',7'-dichlorodihydrofluorescein diacetate (20µM H2DCFDA in culture medium without serum) medium. Cells were incubated for 45 min at 37ºC. H2DCFDA medium was removed and cellswere rinsed with 0.1 M Phosphate Buffered Saline. The cells were harvested from the culture plate by trypsinization (0.25 % Trypsin in PBS) and centrifuged at 1500 rpm for 2 min. The pellet was resuspended in 400µl PBS and 200µl from each sample were transferred to 96 well black plate. Fluorescence intensity was measured using 485 nm excitation and 535 nm filter and percentage ROS activity was calculated using the following equation where RFU = Relative Fluorescence Unit.

$$Percentage\ ROS\ activity = \frac{RFU of test}{RFU of control} \times 100 \qquad \textbf{(4)}$$

3.4 Antibacterial studies

Antimicrobial activity of SPIONs and PLL-coated SPIONs were investigated. The experimental design was towards understanding whether these materials could prevent biofilm formation in both gram-positive and gram-negative bacteria. The ability of these materials to disrupt the biofilm of gram-positive and gram-negative bacteria is also studied.

3.4.1 Biofilm formation

The bacterial strains used for the study was *Pseudomonas aeruginosa* (gram-negative)and *Staphylococcus epidermidis* (gram-positive). The overnight cultures of both bacteria inoculated in tryptone soy broth (TSB) was adjusted to O.D = 1. Mcfarland standard was used here. Then 100µl bacterial suspension was seeded into 96 wellplates and 1000µl TSB was added to it. To observe whether these nanoparticles can prevent the biofilm formation, 25µl aqueous suspension of the nanoparticles were added to this and incubated at 37ºC for 48 hours.

Additionally, for understanding the ability of nanoparticles to disrupt the biofilm, 48 h biofilm of both bacterial strains were exposed to 25µl of the nanoparticle for 24 hours. Controls for all the experiments were*Pseudomonas aeruginosa* and *Staphylococcus epidermidis* cultured for the same duration without nanoparticles.

3.4.2. Crystal Violet Assay

The quantification of the biofilm was done using Crystal Violet (CV) method. The biofilm were stained with 0.1% crystal violet. 1ml of 95% of ethanol was used to dissolve the biofilm-bound CV. The absorbance was measured at 600nm using a microtiter plate reading.

CHAPTER 4

RESULTS AND DISCUSSIONS

This chapter deals with the overall results obtained from the current study followed by possible theoretical interpretation. The synthesis of PLL-modified SPIONs are elaborated in the first section. The next section deals with the characterization techniques. The cell culture works and antibacterial studies are described in subsequent sections.

4.1 Synthesis of Poly-L-Lysine Modified Iron Oxide Nanoparticles

4.1.1 Synthesis of Super Paramagnetic Iron oxide nanoparticles (SPIONs)

Super Paramagnetic Iron oxide nanoparticles were synthesized via co-precipitation method. The obtained nanoparticles were in black colour, well disbursed and showed excellent magnetic properties. Magnetic properties of the synthesized particles were determined using a magnet. SPIONs dispersed in distilled water in the presence and absence of magnetic field are shown in Figure 4.1. The particles thus synthesized were stable upto 3 days after which it showed aggregation.

4.1.2 Synthesis of PLL modified iron oxide nanoparticles

PLL modification SPIONs changed the black colour of the dispersion to brown colour. PLL stabilization is expected to be formed as a result of formation of hydrogen bonded complexes. It is hypothesized that, amine protons present in the PLL chain can form an NH-O bond with the uncoated SPIONs since the surface of bare SPIONs is covered by hydroxyl bond. Also there is a possibility of forming a coordinate bond between carboxyl anions and metal ions.

Among the 5 samples prepared at different concentrations (25µl, 50µl, 100µl, 150µl and 200µl), the sample with concentration 200µl showed greater stability compared to other samples. SPIONs before and after modification with PLL is shown in figure 4.2.

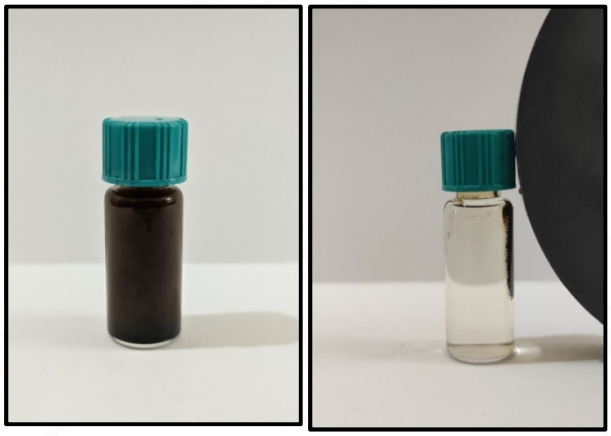

(a) (b)

Figure 4.1 SPIONs (a) before magnetic separation (b) after magnetic separation

(a) **(b)**

Figure 4.2 SPIONs (a) before coating (b) after coating (200µl)

4.2 Characterization of nanoparticles

4.2.1 X-ray diffraction technique (XRD)

The XRD pattern of uncoated SPIONs is shown in figure 4.3-a. The major diffraction peak is observed at 35.23^0(311). In addition to this, there are a number of minor peaks at 30.10^0(220), 42.99^0(400), 53.40^0(422), 56.82^0(511), 62.56^0(440) as per JCPDS card no. 89-0951. This indicates the spinel structure of iron oxide (Fe_3O_4). The XRD data confirms that the synthesized SPIONs do not consist of any other forms of iron oxide in the detectable range.

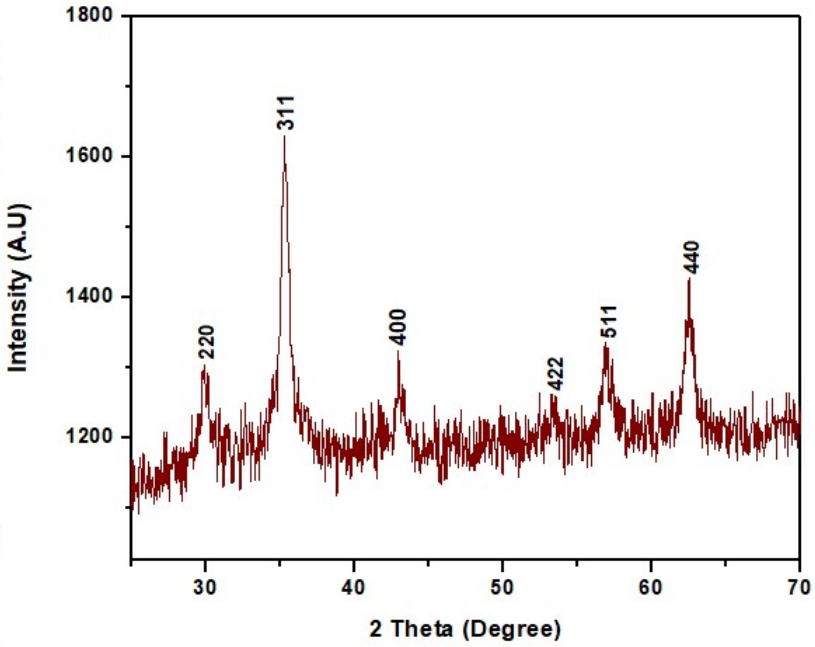

Figure 4.3-a XRD pattern of uncoated SPIONs

The Rietveld refined pattern of the synthesized nanoparticle is shown in figure 4.3-b. In the figure, typical Rietveld fit (red line) is shown over the corresponding raw XRD data (blue dots). The noisy layer(green) is the difference curve between XRD and Rietveld simulation.

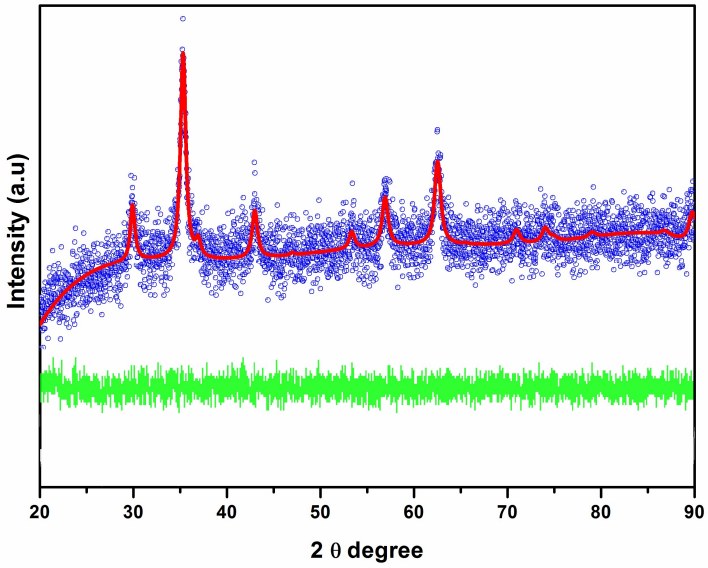

Figure 4.3-b. Rietveld refined pattern of uncoated SPIONs

The reflection positions can be indexed to a single cubic spinel phase which is labeled in the figure. The patterns were refined assuming an inverse spinel crystal structure with Fd3m space group and all Bragg's planes could be indexed to face centered cubic inverse spinel magnetite. Positions of all the peaks are fitted through successive refinements of zero shift error.

Sample Name	Uncoated SPIONs
R_{exp}(%)	2.88
R_{wp}(%)	2.91
R_p(%)	2.31
GOF (%)	1.01
R_{Bragg}(%)	3.263

a (Å)	8.3722
Crytallite size (nm)	14.5
Strain	0.0016

Table 2. The Rietveld parameters obtained from the sample

The lattice constant *a* obtained from refinement is 8.372 (Å) whereas the same for bulk magnetite is 8.396 (Å) (JCPDS card No. 19-0629). All the experimental data could be matched with the theoretical data indicating a good fit. The GoF value remain very close to 1.0. The crystallite size of 14.4nm was obtained from Rietveld analysis. The results thus clearly established that the as synthesized nanoparticle belongs to the magnetite phase. The final values of structural parameters, agreement factors and GoF are listed in Table 2.

4.2.2 Transmission Electron Microscopy

Particle size was analyzed using TEM. TEM image of uncoated and PLL-coated SPIONs are shown in Figure 4.4 and Figure 4.5 respectively.

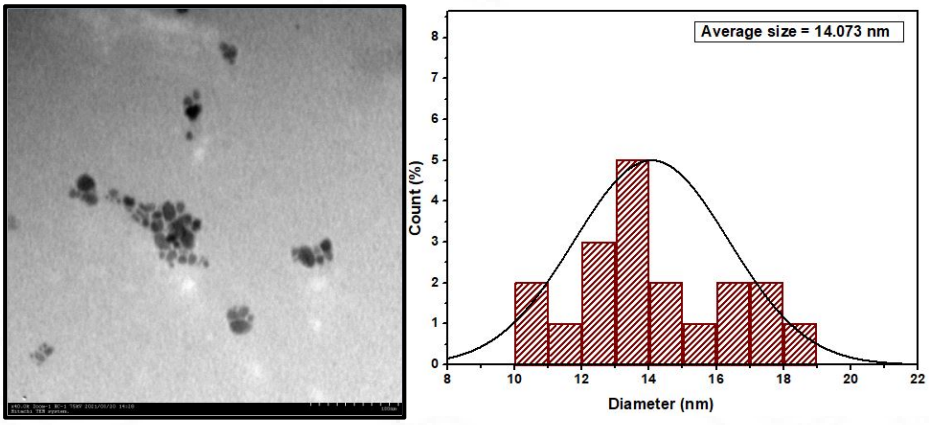

Figure 4.4 TEM micrograph of uncoated SPIONs and calculated histogram with normal fitting

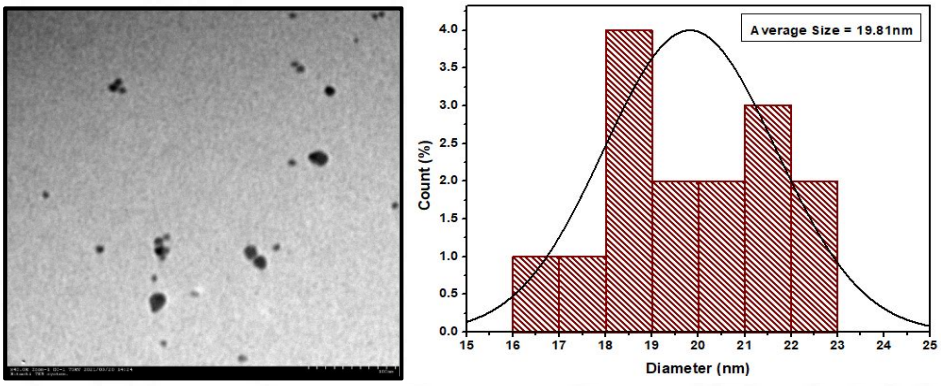

Figure 4.5 TEMmicrograph of PLL-coated SPIONs with calculated histogram with normal fitting

From TEM micrograph, it is clear that, the uncoated SPIONs have a size distribution in the range 14-16 nm with an average diameter 14nm. The PLL-coated SPIONs showed an average size distribution of 18-20 nm. The aggregation has found to be decreased during coating with PLL. Aqueous dispersivity has also increased for PLL-coated SPIONs. The increase in particle size and the reduced aggregation suggest that the SPIONs are well coated with PLL. The particle size

obtained from TEM micrograph agrees well with the data obtained from X-ray diffraction technique.

4.2.3 Dynamic Light Scattering technique (DLS)

Figure 4.6(a) and figure 4.6(b) shows DLS measurements of uncoated SPIONs and PLL-coated SPIONs. The results showed hydrodynamic diameter of 123 nm and 133nm for uncoated SPIONs and PLL-coated SPIONs respectively.

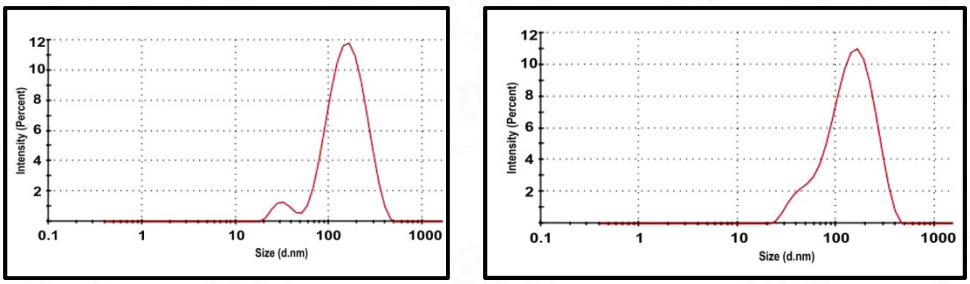

(a) **(b)**

Figure 4.6 Hydrodynamic size distribution of (a) uncoated SPIONs (b) PLL-coated SPIONs

Zeta potential measurements of the synthesized nanoparticles are shown in figure 4.7(a) and figure 4.7 (a). A significant change in the value of potential was observed. The zeta potential varied from 39.6mV to 60.5mV, when SPIONs were coated with PLL. An increase in the zeta potential is due to the amine groups present in PLL. The enhanced zeta potential reflects the stability of the nanomaterials.

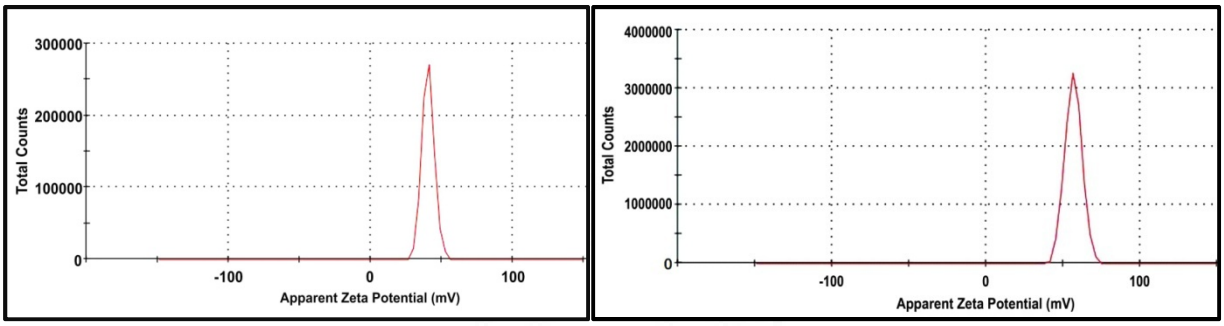

(a) **(b)**

Figure 4.7 Zeta potential measurements of (a) uncoated SPIONs (b) PLL-coated SPIONs

4.2.4 Fourier Transform Infrared Spectroscopy (FTIR)

FTIR spectra of synthesized nanoparticles and PLL are shown in figure 4.8(a-c). The peak at 595cm^{-1} is assigned to Fe-O bond (Figure 4.8-b). Compared to the spectrum of uncoated iron oxide nanoparticles, the PLL coated nanoparticles showed a characteristic peak at 2360cm^{-1} (Figure 4.8-a). This can be due to C-H stretching vibration. The two peaks at 3421cm^{-1} and 3121cm^{-1} can be suggested as the hydroxyl groups (-OH) stretching vibrations and overlap peaks of amine (-NH_2, -NH-). The peak at about 1641cm^{-1} corresponds to the C=O stretching vibrations of amide I group. These results show that SPIONs are coated with PLL.

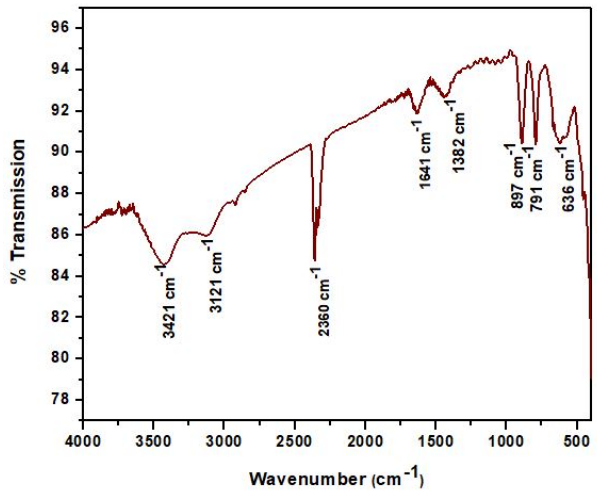

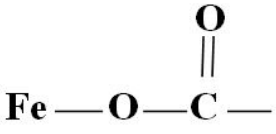

Figure 4.8(a) FTIR spectra of PLL coated SPIONs along with their suggested linkage

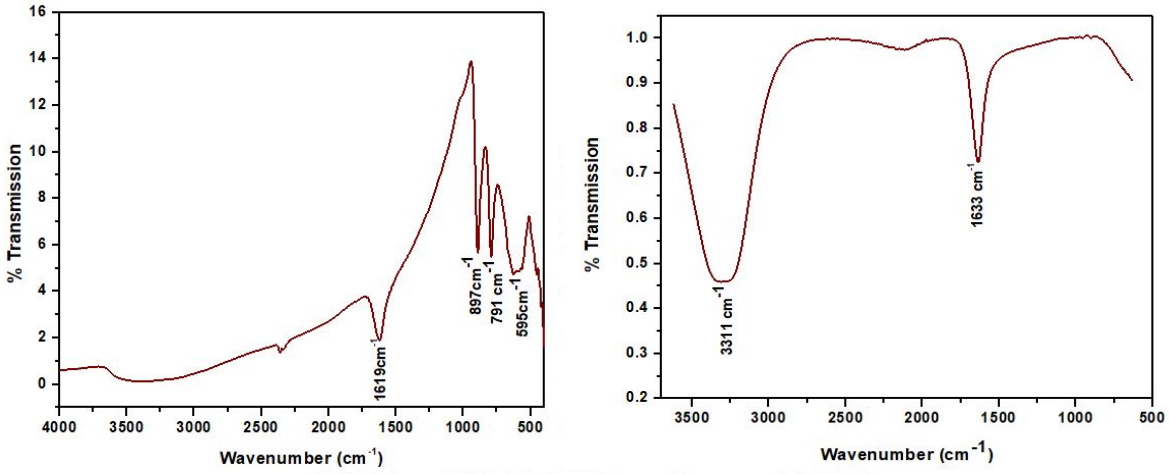

(b) **(c)**

Figure 4.8. FTIR spectrum of (b) uncoated SPIONs (c) PLL

The peak at 595cm^{-1} in the spectrum of uncoated SPIONs was shifted to 636cm^{-1} for PLL-coated SPIONs. As per the theory, the frequency at which a molecule can absorb IR radiation and gets excited is given by equation 5,

$$\vartheta = \frac{1}{2\pi}\left(\frac{k}{\mu}\right)^{\frac{1}{2}} \qquad (5)$$

where ϑ is the wavenumber in cm^{-1}, **k** is the force constant in N/cm and **μ** is the reduced mass in kg.

When the oxygen in the Fe-O bond is bonded with the carbon atom in the PLL chain, the oxygen atom is attracted more towards the Fe atom than the carbon atom since the difference in electronegativity between Fe and O is greater than that between C and O. Even though the reduced mass of Fe and O in Fe-O bond remains same, the bond strengthens and thus the force constant (k) increases. According to equation 3, the wavenumber corresponding to the particular vibration also increases. This can be the reason for the shift of the peak to the longer wavenumber upon coating.

4.3 Cell culture studies

4.3.1 Cytotoxicity assessment

Cytotoxicity of uncoated and PLL-coated SPIONs was evaluated on L929 cell line using MTT assay. There was no difference in cell morphology of cells exposed to uncoated SPIONs(Figure 4.9-a). The culture medium was clear without any precipitate, turbidity or pH change.

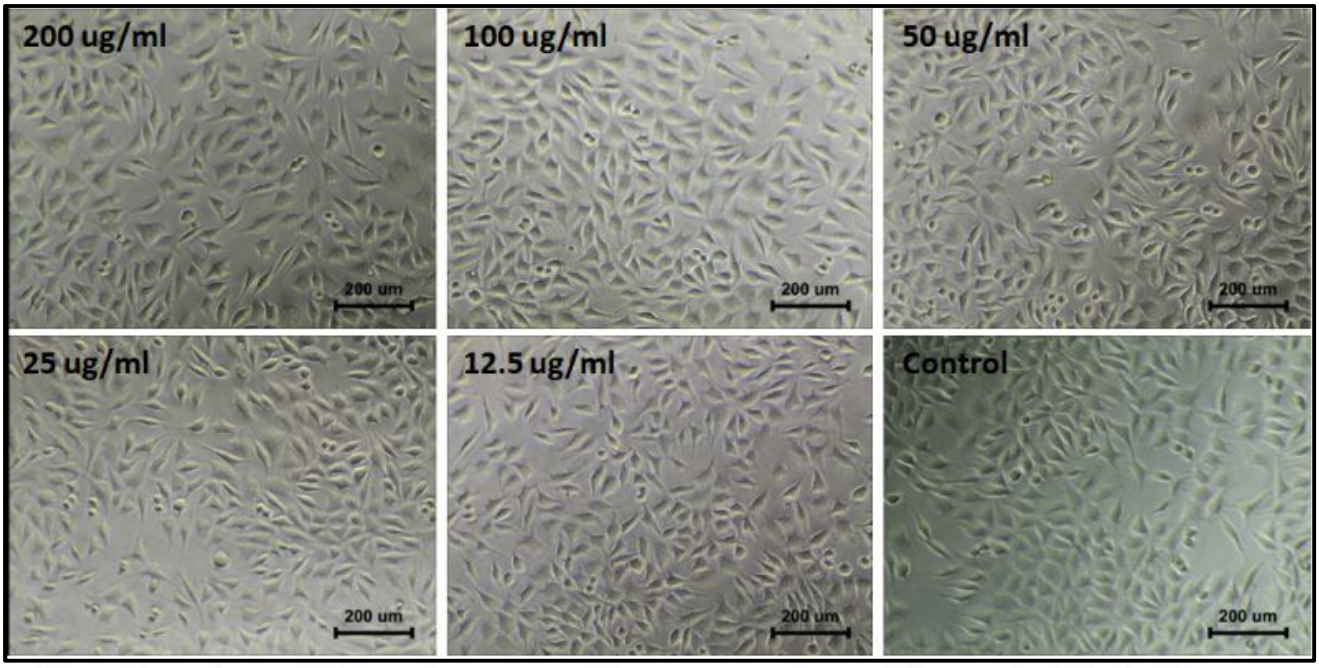

Figure 4.9-a. Cells exposed to different concentrations of uncoated SPIONs

Cells exposed to PLL-coated SPIONs showed dose depended cytotoxicity (Figure 4.9-b). Sample concentration from 25 – 200µg/ml was cytotoxic with evident cell lysis, loss of cell morphology and presence of particulate matter. The dilution of 12.5µg/ml showed similar morphology and culture conditions as in cell control.

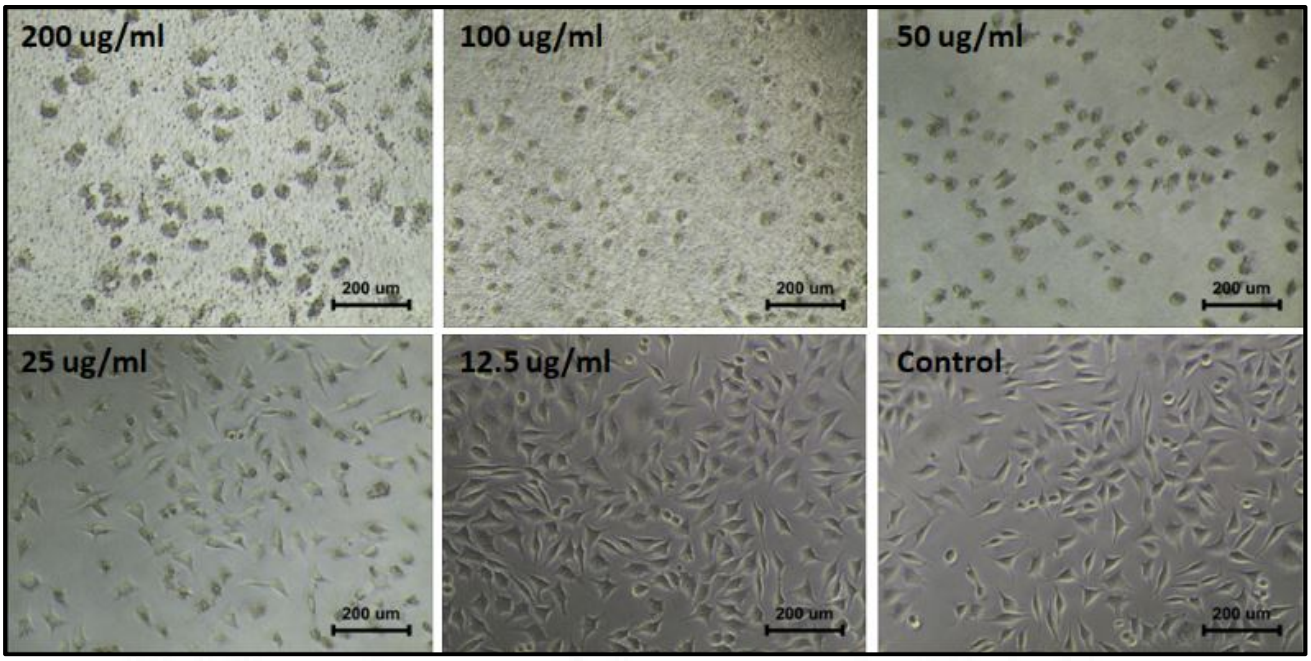

Figure 4.9-b. Cells exposed to different concentrations of PLL-coated SPIONs

4.3.1.1 MTT assay

Percentage cell activity between 61 ± 5 and 78 ± 8 % was obtained for cells exposed to uncoated SPIONs for the concentration range 200, 100, 50, 25, 12.5µg/ml (Figure 4.10-a). For the cells exposed to PLL-coated SPIONs, the concentration from 25 – 200µg/ml was cytotoxic whereas the dilution of 12.5µg/ml was non-cytotoxic (Figure 4.10-b).

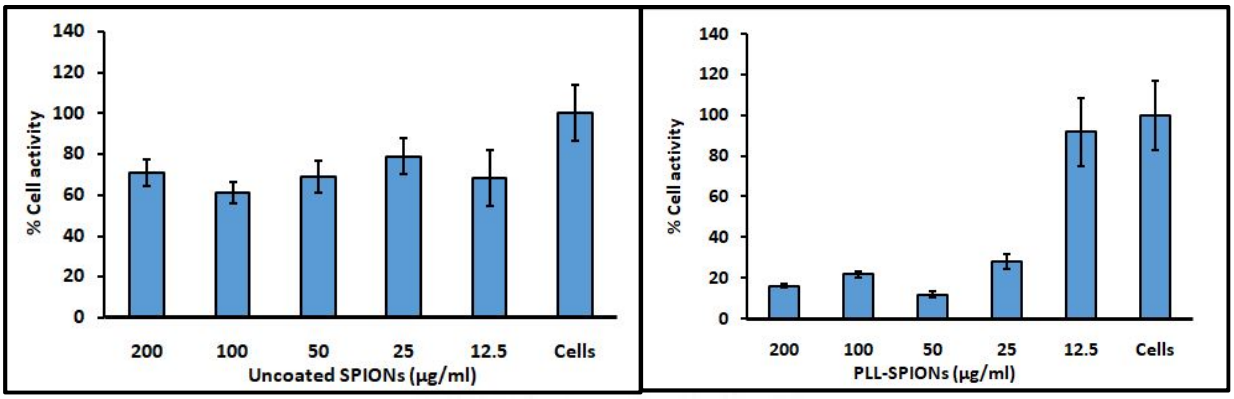

(a) ***(b)***

Figure 4.10. % cell viability for (a) uncoated SPIONs (b) PLL-coated SPIONs

4.3.1.2Half-maximal Inhibitory Concentration (IC50) analysis

The absorbance reading obtained after MTT Assay of PLL-coated SPIONs expressed as log concentration was normalized and then analyzed for the non-linear regression to find inhibitor versus response (Figure 4.11).

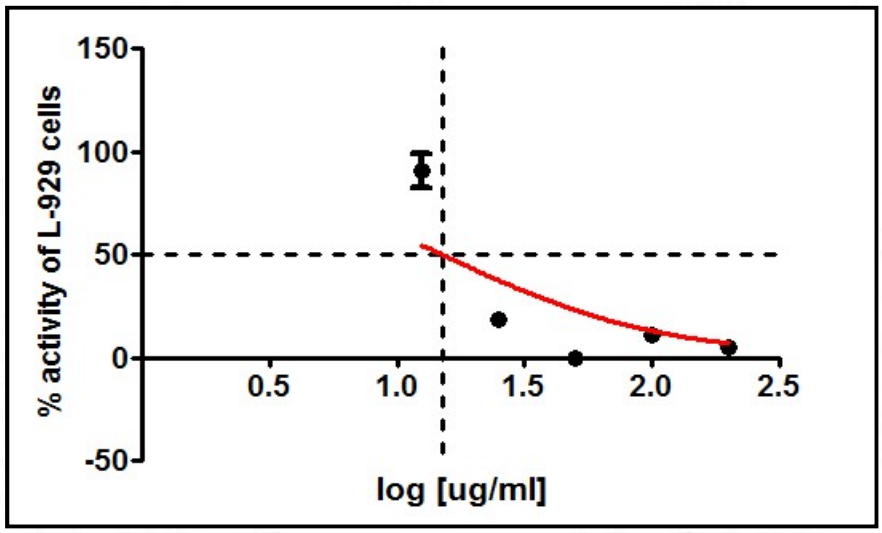

Figure 4.11.IC50 of PLL-coated SPIONs with L-929 cells.

Log IC_{50} value obtained from the graph is 1.17. From IC_{50} value for PLL-coated SPIONs is calculated as 15.7%.Thus, the sample showed IC50 value of 15µg/ml.

4.3.2 H2 DCFDA Assay

Reactive oxygen species (ROS) generated in cells subsequent to exposure of L-929 cells to uncoated SPIONs and PLL coated SPIONs was measured using cell-permeant 2',7'-dichlorodihydrofluorescein diacetate (H2DCFDA) assay. The ROS activity of the synthesized nanoparticles is shown in figure 4.12. Uncoated SPIONs and PLL coated SPIONs are denoted as sample 1 and sample 2 respectively.

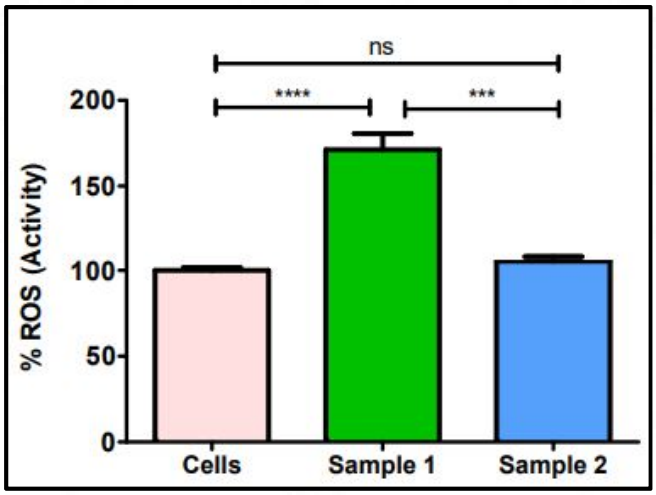

Figure 4.12. ROS assay of L929 cells

The cells exposed to uncoated SPIONs showed intra cellular ROS activity of 171.3 ± 22% compared to cells cultured in normal medium. However, there was no significant difference in the ROS activity between cells exposed to the PLL coated SPIONs (105 ± 5) and the cells cultured in normal medium (100 ± 4).

From the ROS assay, it is evident that, the intracellular ROS activity of SPIONs decreased significantly upon coating with PLL. One of the main drawbacks of SPIONs in which the researchers have pointed out is the generation of ROS in normal cells. It is the main reason for the NP-induced toxicity. In this study it is observed that, PLL coating decreases the free radical

formation. Hence the oxidative stress and DNA damage which are likely to occur while using uncoated SPIONs on normal cells will be less in the case of PLL coated SPIONs.

4.4 Antibacterial studies

The preventive effect of the synthesized nanoparticles on the formation of biofilm of *Pseudomonas aeruginosa* (ATCC 27853) and the disruptive effect on the same on 48 hrs biofilm are shown in Figure 4.13 and Figure 4.14 respectively.

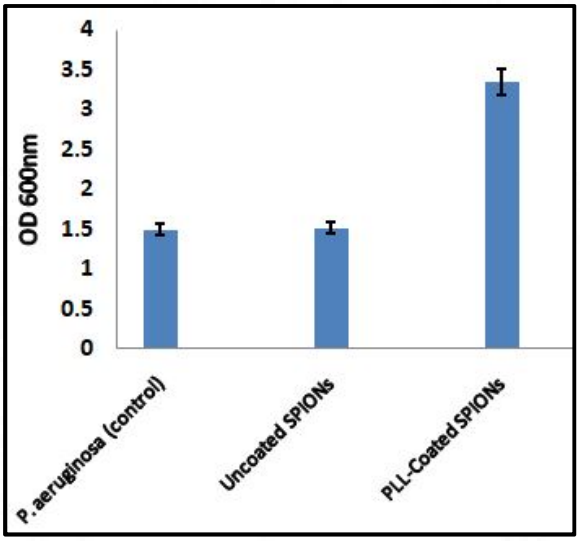

Strain	Mean of three experiments
Pseudomonas aeruginosa(control)	1.489333
Uncoated SPIONs	1.515667
PLL-coated SPIONs	3.343667

Figure 4.13 Effect of NPs to prevent the biofilm formation by *P. aeruginosa*

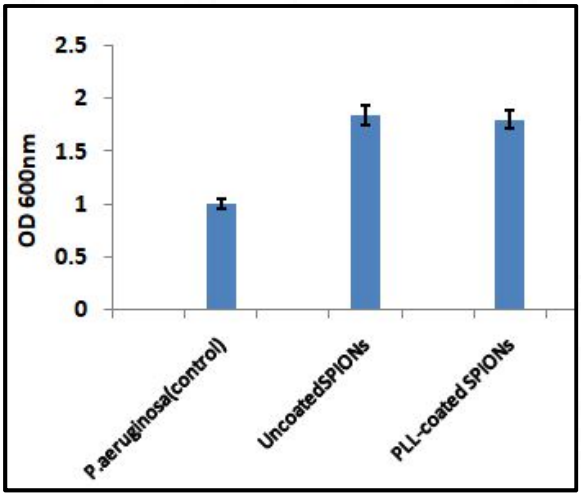

Strain	Mean of three experiments
Pseudomonas aeruginosa(control)	1.002667
Uncoated SPIONs	1.842333
PLL-coated SPIONs	1.806333

Figure 4.14 Effect of NPs to disrupt the biofilm formed by *P. aeruginosa*

Similarly, the preventive effect of the synthesized nanoparticles on the formation of biofilm by *Staphylococcus epidermidis* (ATCC 35984) and the disruptive effect of the same on 48 hrs biofilm are shown in Figure 4.15 and Figure 4.16 respectively

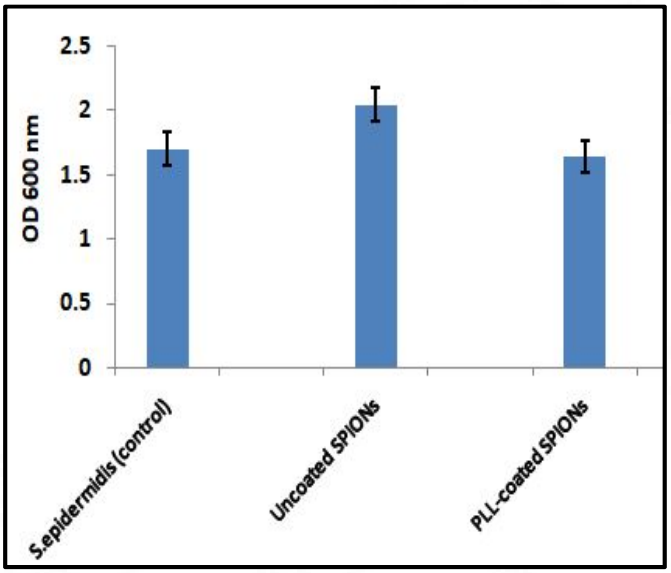

Strain	Mean of three experiments
Staphylococcus epidermidis (control)	1.704667
Uncoated SPIONs	2.05
PLL-coated SPIONs	1.647

Figure 4.15. Effect of NPs to prevent the biofilm formation by *S. epidermidis*

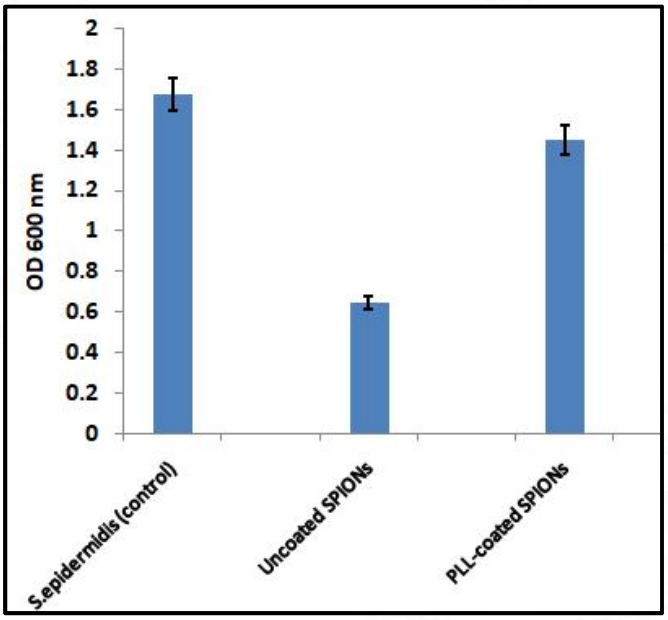

Strain	Mean of three experiments
Staphylococcus epidermidis (control)	1.675667
Uncoated SPIONs	0.644
PLL-coated SPIONs	1.448667

Figure 4.16. Effect of NPs to disrupt the biofilm formed by *S. epidermidis*

The effect of synthesized nanoparticles on biofilm formation was evaluated using crystal violet assay at a concentration of 25µl and the respective data are shown. In this initial preliminary study using lower levels of concentration, uncoated and PLL-coated SPIONs showed no antibiofilm properties for both gram-positive and gram-negative bacteria.

However, biofilm formed in 48 hrs, the nanomaterials showed encouraging results on the antibiofilm activity for the gram-positive bacterial strain. Uncoated SPIONs exhibited a significant antibiofilm effect compared to their PLL-coated counterparts. The increased antibiofilm effect can be attributed to the production of ROS within the bacterial cells in the presence of nanoparticles.

CHAPTER 5

SUMMARY AND CONCLUSIONS

5.1 SUMMARY

Bacterial colonization and biofilm formation is a growing concern for most of the healthcare providers across the globe. Even though many antibiotics are available, none of them offer a complete solution towards biofilm destruction since antibiotic-resistant bacteria are very common. The need of the hour is to develop novel antimicrobial agents and antibiofilm surfaces to overcome this issue. Nanotechnology has opened new ways to cop up with this problem. This study focuses on these problems to a great extent.

It is well established that surface modification of SPIONs with a suitable polymer can reduce nanoparticle-induced toxicity. Based on this knowledge we hypothesized that appropriately chosen polymer coating could be capable of disrupting the bacterial biofilm completely. Based on this hypothesis, the major objectives of the current study are to synthesize super paramagnetic iron oxide nanoparticles (SPIONs) and modify them with Poly-L-lysine (PLL), a biocompatible polymer to enhance its antibacterial properties. The other objective was to evaluate the antibiofilm properties of the synthesized material using gram-negative and gram-positive bacteria.

SPIONs were synthesized through chemical co-precipitation route in the presence of NaOH. Nanoparticles of average size distribution 14-15 nm were obtained. The size was further confirmed from XRD data. The XRD pattern reveals the magnetite phase of the SPIONs. The uncoated SPIONs were modified by PLL. The size and shape of synthesized nanoparticles were obtained from TEM analysis. DLS technique was employed to analyze the hydrodynamic

diameter of the synthesized nanoparticles. The shift in the peaks was observed in FTIR spectrum of PLL-coated SPIONs compared to that of uncoated SPIONs and PLL alone. The shift in the band towards longer wavelength is attributed to the strengthening of Fe-O bond followed by the increase in force constant between them.

Cytotoxicity studies were carried out to evaluate the toxic levels of synthesized nanomaterial. From MTT assay it was clear that, the PLL-coated SPIONs showed a dose-dependent toxicity and uncoated SPIONs showed no cytotoxicity over the range of measured concentrations. H2DCFDA assay showed that, the ROS generation was reduced upon coating. Antibacterial studies were done to estimate the biofilm capacity of the synthesized nanoparticles. The bacterial strains used for the study were *Pseudomonas aeruginosa* and *Staphylococcus epidermidis*. The biofilm growth was quantified using crystal violet assay. It was seen that at lower concentrations, there was no significant antibacterial property for both coated and uncoated nanoparticles.

5.2 CONCLUSIONS

The PLL modified SPIONs were successfully synthesized and characterized. The synthesized nanoparticles were found to have excellent magnetic properties and stability. XRD and TEM data confirmed the particle size and shape of the synthesized nanoparticles. The average diameter of the nanoparticles were obtained as 14nm. Prior to polymer coating, the SPIONs showed aggregation. TEM images indicated that, the polymer coating have decreased the agglomeration significantly. The coating of PLL on SPIONs was further confirmed from DLS data and FTIR spectrum. Upon coating, Fe-O bond strengthening was observed by analyzing the peak shift from FTIR spectrum. Increase in the zeta potential is also an indication

of PLL coating on SPIONs. Enhancement in zeta potential is assumed to favour the antimicrobial action of PLL-coated SPIONs.

MTT assay showed a dose-dependent cytotoxicity for PLL-modified SPIONs where as uncoated SPIONs were non-cytotoxic for all the measured concentration range. From H2DCFDA assay, it was clear that, the polymer coating has reduced ROS production considerably.

In the preliminary studies, the biofilm quantification was done using crystal violet assay. It was clear that the PLL-coated SPIONs have no significant antibacterial property at lower concentrations. A dose-dependent reduction in bacterial biomass is expected for the synthesized nanoparticles, for which inhibitory concentration of the nanoparticles after assessing multiple concentrations has to be finalised.

FUTURE PROSPECTS

In the present study, biofilm quantification was done using crystal violet assay for a single concentration value. Future studies will includeevaluation of the antibiofilm properties of the synthesized nanoparticles over a wide range of concentrations. Membrane integrity and the structure of the biofilm will be observed using different techniques like ESEM, which will provide a complete understanding on the proposed mechanism. To further confirm the results obtained, DCFDA assay willalso be performed on bacterial cells .The relation between magnetic properties of PLL-coated SPIONs and their antibacterial properties is not well studied in the present study. The magnetic properties of the nanoparticles have to be evaluated in detail to understand the mechanism of the decreased ROS generation and the exhibited antimicrobial properties.

REFERENCES

1. Abakumov, M. A., Semkina, A. S., Skorikov, A. S., Vishnevskiy, D. A., Ivanova, A. V., Mironova, E., Chekhonin, V. P. (2018). Toxicity of iron oxide nanoparticles: Size and coating effects. *Journal of Biochemical and Molecular Toxicology*, *32*(12). https://doi.org/10.1002/jbt.22225

2. Ajinkya, N., Yu, X., Kaithal, P., Luo, H., Somani, P., & Ramakrishna, S. (2020). Magnetic iron oxide nanoparticle (IONP) synthesis to applications: Present and future. *Materials*, *13*(20), 1–35. https://doi.org/10.3390/ma13204644

3. Ansari, M. A., Khan, H. M., Khan, A. A., Cameotra, S. S., Saquib, Q., & Musarrat, J. (2014). Interaction of Al_2O_3 nanoparticles with Escherichia coli and their cell envelope biomolecules. *Journal of Applied Microbiology*, *116*(4), 772–783. https://doi.org/10.1111/jam.12423

4. Arakha, M., Pal, S., Samantarrai, D., Panigrahi, T. K., Mallick, B. C., Pramanik, K., Mallick, B., & Jha, S. (2015). Antimicrobial activity of iron oxide nanoparticle upon modulation of nanoparticle-bacteria interface. *Scientific Reports*, *5*, 1–12. https://doi.org/10.1038/srep14813

5. Arias, L. S., Pessan, J. P., Vieira, A. P. M., De Lima, T. M. T., Delbem, A. C. B., & Monteiro, D. R. (2018, June 9). Iron oxide nanoparticles for biomedical applications: A perspective on synthesis, drugs, antimicrobial activity, and toxicity. *Antibiotics*. MDPI AG. https://doi.org/10.3390/antibiotics7020046

6. Armijo, L. M., Wawrzyniec, S. J., Kopciuch, M., Brandt, Y. I., Rivera, A. C., Withers, N. J., Cook, N. C., Huber, D. L., Monson, T. C., Smyth, H. D. C., & Osiński, M. (2020).

Antibacterial activity of iron oxide, iron nitride, and tobramycin conjugated nanoparticles against Pseudomonas aeruginosa biofilms. *Journal of Nanobiotechnology*, *18*(1), 1–27. https://doi.org/10.1186/s12951-020-0588-6

7. Attucci, S. (n.d.). *Poly- L -Lysine Compacts DNA , Kills Bacteria , and Improves Protease Inhibition in Cystic Fibrosis Sputum*. *3*(9). https://doi.org/10.1164/rccm.201305-0912OC

8. Babič, M., Horák, D., Trchová, M., Jendelová, P., Glogarová, K., Lesný, P., Herynek, V., Hájek, M., & Syková, E. (2008). Poly(L-lysine)-modified iron oxide nanoparticles for stem cell labeling. *Bioconjugate Chemistry*, *19*(3), 740–750. https://doi.org/10.1021/bc700410z

9. Bei, Y. (2017. Nanocatalysts. HHS Public Access. *Physiology & Behavior*, *176*(3), 139–148. https://doi.org/10.1016/j.biomaterials.2016.05.051.

10. Bondarenko, L. S., Kovel, E. S., Kydralieva, K. A., Dzhardimalieva, G. I., Illés, E., Tombácz, E., Kicheeva, A. G., & Kudryasheva, N. S. (2020). Effects of modified magnetite nanoparticles on bacterial cells and enzyme reactions. *Nanomaterials*, *10*(8), 1–20. https://doi.org/10.3390/nano10081499

11. Bondarenko, L. S., Kovel, E. S., Kydralieva, K. A., Dzhardimalieva, G. I., Illés, E., Tombácz, E., Kicheeva, A. G., & Kudryasheva, N. S. (2020). Effects of modified magnetite nanoparticles on bacterial cells and enzyme reactions. *Nanomaterials*, *10*(8), 1–20. https://doi.org/10.3390/nano10081499

12. Boudarel, H., Mathias, J. D., Blaysat, B., & Grédiac, M. (2018). Towards standardized mechanical characterization of microbial biofilms: analysis and critical review. *Npj Biofilms and Microbiomes*, *4*(1). https://doi.org/10.1038/s41522-018-0062-5

13. Dadashi, S., Poursalehi, R., & Delavari, H. (2015). Structural and Optical Properties of Pure Iron and Iron Oxide Nanoparticles Prepared via Pulsed Nd:YAG Laser Ablation in Liquid. *Procedia Materials Science*, *11*, 722–726. https://doi.org/10.1016/j.mspro.2015.11.052

14. Ding, W., Ma, C., Zhang, W., Chiang, H., Tam, C., Xu, Y., Zhang, G., & Qian, P. Y. (2018). Anti-biofilm effect of a butenolide/polymer coating and metatranscriptomic analyses. *Biofouling*, *34*(1), 111–122. https://doi.org/10.1080/08927014.2017.1409891

15. Ebrahiminezhad, A., Ghasemi, Y., Rasoul-Amini, S., Barar, J., & Davaran, S. (2012). Impact of amino-acid coating on the synthesis and characteristics of iron-oxide nanoparticles (IONs). *Bulletin of the Korean Chemical Society*, *33*(12), 3957–3962. https://doi.org/10.5012/bkcs.2012.33.12.3957

16. Ebrahiminezhad, A., Varma, V., Yang, S., Ghasemi, Y., & Berenjian, A. (2015). Synthesis and application of amine functionalized iron oxide nanoparticles on menaquinone-7 fermentation: A step towards process intensification. *Nanomaterials*, *6*(1), 1–9. https://doi.org/10.3390/nano6010001

17. Feldman, M., Sionov, R., Smoum, R., Mechoulam, R., Ginsburg, I., & Steinberg, D. (2020). Comparative Evaluation of Combinatory Interaction between Endocannabinoid System Compounds and Poly-L-lysine against Streptococcus mutans Growth and Biofilm Formation. *BioMed Research International*, *2020*. https://doi.org/10.1155/2020/7258380

18. Gabrielyan, L., Hovhannisyan, A., Gevorgyan, V., Ananyan, M. & Trchounian, A. Antibacterial effects of iron oxide (Fe3O4) nanoparticles: distinguishing concentration-

dependent effects with different bacterial cells growth and membrane-associated mechanisms. *Applied Microbiology and Biotechnology* **103,** 2773–2782 (2019).

19. Gabrielyan, L., Hovhannisyan, A., Gevorgyan, V., Ananyan, M., & Trchounian, A. (2019). Antibacterial effects of iron oxide (Fe 3 O 4) nanoparticles: distinguishing concentration-dependent effects with different bacterial cells growth and membrane-associated mechanisms. *Applied Microbiology and Biotechnology*, *103*(6), 2773–2782. https://doi.org/10.1007/s00253-019-09653-x

20. Gao, L., Fan, K., & Yan, X. (2017). Iron oxide nanozyme: A multifunctional enzyme mimetic for biomedical applications. *Theranostics*. Ivyspring International Publisher. https://doi.org/10.7150/thno.19738

21. Gao, L., Liu, Y., Kim, D., Li, Y., Hwang, G., Naha, P. C., Cormode, D. P., & Koo, H. (2016). Nanocatalysts promote Streptococcus mutans biofilm matrix degradation and enhance bacterial killing to suppress dental caries in vivo. *Biomaterials*, *101*, 272–284. https://doi.org/10.1016/j.biomaterials.2016.05.051

22. https://doi.org/10.3389/fncel.2017.00083

23. Hyldgaard, M., Mygind, T., Vad, B. S., Stenvang, M., Otzen, D. E., & Meyer, R. L. (2014). The antimicrobial mechanism of action of epsilon-poly-L-lysine. *Applied and Environmental Microbiology*, *80*(24), 7758–7770. https://doi.org/10.1128/AEM.02204-14

24. Khatoon, Z., McTiernan, C. D., Suuronen, E. J., Mah, T. F., & Alarcon, E. I. (2018, December 1). Bacterial biofilm formation on implantable devices and approaches to its treatment and prevention. *Heliyon*. Elsevier Ltd. https://doi.org/10.1016/j.heliyon.2018.e01067

25. L, E. T. P.-, Guillon, A., Fouquenet, D., Morello, E., Henry, C., Georgeault, S., & Si-tahar, M. (2018). *crossm Treatment of Pseudomonas aeruginosa Biofilm Present in*. *62*(11), 1–10.

26. Li, L., Jiang, W., Luo, K., Song, H., Lan, F., Wu, Y., & Gu, Z. (2013). Superparamagnetic iron oxide nanoparticles as MRI contrast agents for non-invasive stem cell labeling and tracking. *Theranostics*, *3*(8), 595–615. https://doi.org/10.7150/thno.5366

27. Liu, Y. ScholarlyCommons Dextran-coated Iron Oxide Nanoparticles as Biomimetic Catalysts for Biofilm Disruption and Caries Prevention Dextran-coated Iron Oxide Nanoparticles as Biomimetic Catalysts for Biofilm. (2019).

28. Louro H. (2018) Relevance of Physicochemical Characterization of Nanomaterials for Understanding Nano-cellular Interactions. In: Saquib Q., Faisal M., Al-Khedhairy A., Alatar A. (eds) Cellular and Molecular Toxicology of Nanoparticles. Advances in Experimental Medicine and Biology, vol 1048. Springer, Cham. https://doi.org/10.1007/978-3-319-72041-8_8

29. Mahmoudi, M., Simchi, A., Imani, M., Milani, A. S., & Stroeve, P. (2009). An in vitro study of bare and poly(ethylene glycol)-co-fumarate-coated superparamagnetic iron oxide nanoparticles: A new toxicity identification procedure. *Nanotechnology*, *20*(22). https://doi.org/10.1088/0957-4484/20/22/225104

30. Narayana, S. V. V. S. P. (2019). *A Review on Surface Modifications and Coatings on Implants to Prevent Biofilm*.

31. Nikolova, M. P., & Chavali, M. S. (2020). Metal Oxide Nanoparticles as Biomedical Materials. *Biomimetics (Basel, Switzerland)*, *5*(2), 27. https://doi.org/10.3390/biomimetics5020027

32. O'Toole, G. A., & Kolter, R. (1998). Initiation of biofilm formation in Pseudomonas fluorescens WCS365 proceeds via multiple, convergent signalling pathways: A genetic analysis. *Molecular Microbiology*, *28*(3), 449–461. https://doi.org/10.1046/j.1365-2958.1998.00797.x

33. P., S. V. V. S. N., & P., S. V. V. S. (2019). A Review on Surface Modifications and Coatings on Implants to Prevent Biofilm. Regenerative Engineering and Translational Medicine. doi:10.1007/s40883-019-00116-3.

34. Predescu, A. M., Matei, E., Berbecaru, A. C., Pantilimon, C., Drăgan, C., Vidu, R., Predescu, C., & Kuncser, V. (2018). Synthesis and characterization of dextran-coated iron oxide nanoparticles. *Royal Society Open Science*, *5*(3). https://doi.org/10.1098/rsos.171525

35. Prodan, A. M., Iconaru, S. L., Ciobanu, C. S., Chifiriuc, M. C., Stoicea, M., & Predoi, D. (2013). Iron oxide magnetic nanoparticles: Characterization and toxicity evaluation by in vitro and in vivo assays. *Journal of Nanomaterials*, *2013*. https://doi.org/10.1155/2013/587021

36. Raghunath, A., & Perumal, E. (2017). Metal oxide nanoparticles as antimicrobial agents: a promise for the future. *International Journal of Antimicrobial Agents*, *49*(2), 137–152. https://doi.org/10.1016/j.ijantimicag.2016.11.011

37. Raja, P. M. V., & Barron, A. R. (2021, March 21). Zeta Potential Analysis. Retrieved June 7, 2021, from https://chem.libretexts.org/@go/page/55842

38. Sánchez-López, E., Gomes, D., Esteruelas, G., Bonilla, L., Lopez-Machado, A. L., Galindo, R., Cano, A., Espina, M., Ettcheto, M., Camins, A., Silva, A. M., Durazzo, A., Santini, A., Garcia, M. L., & Souto, E. B. (2020). Metal-Based Nanoparticles as Antimicrobial Agents: An Overview. *Nanomaterials (Basel, Switzerland)*, *10*(2), 292. https://doi.org/10.3390/nano10020292

39. Sathyanarayanan, M. B., Balachandranath, R., Genji Srinivasulu, Y., Kannaiyan, S. K., & Subbiahdoss, G. (2013). The Effect of Gold and Iron-Oxide Nanoparticles on Biofilm-Forming Pathogens. *ISRN Microbiology*, *2013*, 1–5. https://doi.org/10.1155/2013/272086

40. Search, H., Journals, C., Contact, A., Iopscience, M., & Address, I. P. (2003). *Applications of magnetic nanoparticles in biomedicine*. *167*.

41. Shkodenko, L., Kassirov, I., & Koshel, E. (2020). Metal oxide nanoparticles against bacterial biofilms: Perspectives and limitations. *Microorganisms*, *8*(10), 1–21. https://doi.org/10.3390/microorganisms8101545

42. Thukkaram, M., Sitaram, S., Kannaiyan, S. K., & Subbiahdoss, G. (2014). Antibacterial efficacy of iron-oxide nanoparticles against biofilms on different biomaterial surfaces. *International Journal of Biomaterials*, *2014*. https://doi.org/10.1155/2014/716080

43. Tinkle, S., McNeil, S. E., Mühlebach, S., Bawa, R., Borchard, G., Barenholz, Y. C., et al. (2014). Nanomedicines: addressing the scientific and regulatory gap. *Ann. N. Y. Acad. Sci.* 1313, 35–56. doi: 10.1111/nyas.12403

44. Trafny, E. A. (2008). Biofilms and their role in infection pathogenesis. *Postepy Mikrobiologii*, *47*(3).

45. Tribedi, P., Sil, A.K. Low-density polyethylene degradation by *Pseudomonas* sp. AKS2 biofilm. *Environ Sci Pollut Res* **20,** 4146–4153 (2013). https://doi.org/10.1007/s11356-012-1378-y

46. Vallabani, N., Karakoti, A. S., & Singh, S. (2017). ATP-mediated intrinsic peroxidase-like activity of Fe_3O_4-based nanozyme: One step detection of blood glucose at physiological pH. *Colloids and surfaces. B, Biointerfaces*, *153*, 52–60. https://doi.org/10.1016/j.colsurfb.2017.02.004

47. Wei, L., Wu, R., Wang, C., & Wu, Z. (2017). Effects of ε-polylysine on pseudomonas aeruginosa and aspergillus fumigatus biofilm in vitro. *Medical Science Monitor*, *23*, 4225–4229. https://doi.org/10.12659/MSM.903145

48. Wilczewska, A. Z., Misztalewska, I., Mys-, J., Michalak, G., Sodo, A., Watek, M., & Stanisław, G. (2016). NU. *Nanomedicine: Nanotechnology, Biology, and Medicine*. https://doi.org/10.1016/j.nano.2016.07.006

49. Yang, G., Zhang, B., Wang, J., Xie, S., & Li, X. (2015). Preparation of polylysine-modified superparamagnetic iron oxide nanoparticles. *Journal of Magnetism and Magnetic Materials*, *374*, 205–208. https://doi.org/10.1016/j.jmmm.2014.08.040

50. Ye, R., Xu, H., Wan, C., Peng, S., Wang, L., Xu, H., Aguilar, Z. P., Xiong, Y., Zeng, Z., & Wei, H. (2013). Antibacterial activity and mechanism of action of ε-poly-l-lysine. *Biochemical and Biophysical Research Communications*, *439*(1), 148–153. https://doi.org/10.1016/j.bbrc.2013.08.001

51. Zheng, M., Pan, M., Zhang, W., Lin, H., Wu, S., Lu, C., Tang, S., Liu, D., & Cai, J. (2021). Poly(α-L-lysine)-based nanomaterials for versatile biomedical applications:

Current advances and perspectives. *BioactiveMaterials*, *6*(7), 1878–1909. https://doi.org/10.1016/j.bioactmat.2020.12.001

52. Zhu, N.; Ji, H.; Yu, P.; Niu, J.; Farooq, M.U.; Akram, M.W.; Udego, I.O.; Li, H.; Niu, X. Surface Modification of Magnetic Iron Oxide Nanoparticles. *Nanomaterials* **2018**, *8*, 810. https://doi.org/10.3390/nano8100810